

OPEN ACCESS

EDITED BY

Choong-Min Ryu, Korea Research Institute of Bioscience and Biotechnology (KRIBB), Republic of Korea

REVIEWED BY

Giulia Malacarne, Fondazione Edmund Mach, Italy Eduardo Valencia-Cantero, Michoacana University of San Nicolás de Hidalgo, Mexico

*CORRESPONDENCE
Estrella Luna

☑ e.lunadiez@bham.ac.uk
Chiara Murena
☑ up202109153@up.pt

RECEIVED 29 July 2025
ACCEPTED 09 September 2025
PUBLISHED 26 September 2025

CITATION

Murena C, Pastor V, Fernandes TR, Carvalho SMP and Luna E (2025) Unravelling induced resistance in strawberry: distinct metabolomic signatures define cultivarspecific resistance to *Botrytis cinerea*. *Front. Plant Sci.* 16:1675649. doi: 10.3389/fpls.2025.1675649

COPYRIGHT

© 2025 Murena, Pastor, Fernandes, Carvalho and Luna. This is an open-access article distributed under the terms of the Creative Commons Attribution License (CC BY). The use, distribution or reproduction in other forums is permitted, provided the original author(s) and the copyright owner(s) are credited and that the original publication in this journal is cited, in accordance with accepted academic practice. No use, distribution or reproduction is permitted which does not comply with these terms.

Unravelling induced resistance in strawberry: distinct metabolomic signatures define cultivar-specific resistance to *Botrytis cinerea*

Chiara Murena^{1*}, Victoria Pastor², Tânia R. Fernandes¹, Susana M. P. Carvalho¹ and Estrella Luna^{3*}

¹GreenUPorto - Sustainable Agrifood Production Research Centre/Inov4Agro, Departamento de Geociências, Ambiente e Ordenamento do Território (DGAOT), Faculty of Sciences, University of Porto, Vairão, Portugal, ²Department of Biology, Biochemistry, and Natural Sciences, School of Technology and Experimental Sciences, Universitat Jaume I, Castelló de la Plana, Spain, ³School of Biosciences, University of Birmingham, Birmingham, United Kingdom

Introduction: Botrytis cinerea is a major pathogen in strawberry, and sustainable alternatives to fungicides are needed to manage this disease. Induced resistance (IR) through chemical elicitors represents a promising strategy, but the effectiveness of such compounds remains poorly understood in commercial strawberry (Fragaria × ananassa) cultivars.

Methods: In this study, we evaluated the efficacy of repeated applications of five elicitors (*i.e.*, β -aminobutyric acid (BABA), (R)- β -homoserine (RBH), indole-3-carboxylic acid (I3CA), jasmonic acid (JA), and salicylic acid (SA)) in three strawberry cultivars (Rowena, Soraya, and Durban).

Results: BABA and RBH significantly reduced *B. cinerea* lesion sizes in Rowena and Soraya, while Durban showed no induced resistance to the elicitors. Untargeted metabolomic profiling of Rowena and Soraya revealed cultivarspecific responses to elicitor treatment and infection, with distinct patterns of metabolite accumulation under both mock- and *B. cinerea*-inoculated conditions. RBH in Rowena and BABA in Soraya induced the most extensive priming-associated metabolic reprogramming, including enrichment of amino acid, nucleotide, and secondary metabolite pathways such as flavonoids and phenylpropanoids. Significantly, none of the elicitors negatively affected plant growth, flowering, or fruit set.

Discussion: These results demonstrate that the effectiveness and mechanism of IR in strawberry depend on both the elicitor and the cultivar, providing new insights into the metabolomic basis of priming with implications for sustainable disease management in strawberry cultivation.

KEYWORDS

grey mould, chemical elicitors, phytohormones, crop protection, β -aminobutyric acid, R- β -homoserine, Fragaria x ananassa

Introduction

The necrotrophic fungus Botrytis cinerea, the causal agent of grey mould disease, is among the most economically damaging pathogens affecting strawberry plants (Fragaria × ananassa Duch.; Family: Rosaceae) (Petrasch et al., 2019). Strawberries are a significant global commodity, with an annual production of approximately 10 million tons worldwide (FAO, U. W., and WOAH, 2023). However, this productivity is severely threatened because of the crop's high susceptibility to B. cinerea (Bestfleisch et al., 2015). Grey mould manifests as necrotic lesions that rapidly develop into water-soaked areas, where the fungus spreads, producing dense mycelial growth and spores, ultimately leading to the collapse of the affected organs (Williamson et al., 2007). It is estimated that over half of the strawberry yield can be lost at postharvest if plants are not treated with fungicides before the harvest (Hassan et al., 2021; Petrasch et al., 2019). Despite the emergence of B. cinerea-resistant strains and the potential adverse effects on human health and the environment, chemical fungicides remain widely used due to their high efficacy (Chen et al., 2016). Consequently, it is crucial to develop new sustainable chemical alternatives to reduce B. cinerea incidence in strawberry. A deeper understanding of strawberry defence responses to B. cinerea is therefore essential. One promising strategy for sustainable crop protection is harnessing the plant immune responses using naturally derived compounds to stimulate Induced Resistance (IR). When exposed to local and temporary stress stimuli, plants can develop an IR phenotype, characterized by enhanced defence capacity and reduced susceptibility to future challenges (De Kesel et al., 2021). This response may involve direct activation of defences, which can impose severe plant fitness costs due to the constant expression of defence mechanisms, or a more energy-efficient process known as priming, where plants, after the perception of a first stimulus, are sensitised to respond more rapidly and strongly to subsequent attacks (He et al., 2022; Mauch-Mani et al., 2017; van Hulten et al., 2006). Priming is particularly attractive as it offers the benefits of enhanced defences with minimal fitness costs (Martinez-Medina et al., 2016). It can be long-lasting, creating a durable immunological memory that is maintained throughout the plant's life cycle and even transmitted across generations, being particularly relevant for vegetatively propagated crops (Catoni et al., 2022), such as strawberry. Several exogenous chemical agents, known as elicitors, can trigger IR and prime the plant's defences. For instance, the application of the phytohormones jasmonic acid (JA) and salicylic acid (SA) can prime plant defences (Pastor et al., 2013). Typically, JA mediates defence against necrotrophic pathogens, while SA is more effective against biotrophs (Ghozlan et al., 2020; Liao et al., 2022). JA has successfully primed tomato defences against B. cinerea when applied to seeds or seedlings, without causing any growth reduction (Luna, 2016; Worrall et al., 2012). On the contrary, the role of SA in defence against B. cinerea is unclear. While beneficial effects were observed following the application of SA in tomato (Li and Zou, 2017), pepper (Mekawi

et al., 2019), and strawberry (Babalar et al., 2007), enhanced susceptibility was also reported (El Oirdi et al., 2011; Fugate et al., 2013; Ha et al., 2021; Khanam et al., 2005). The contradictory findings, together with the limited investigation of JA and SA as preharvest treatments, highlight the necessity for specific case studies within the B. cinerea-strawberry pathosystem (Koo et al., 2020). The non-protein amino acid β-aminobutyric acid (BABA) has emerged as a potent chemical priming agent. Once considered a xenobiotic, BABA has recently been identified as a natural plant metabolite involved in stress signalling (Thevenet et al., 2017). BABA induces broad-spectrum resistance by priming multiple signalling pathways, including both SA-dependent (Zimmerli et al., 2001) and SA-independent mechanisms (Ton and Mauch-Mani, 2004). In Arabidopsis thaliana, activation of defence-related pathways is mediated by binding of the active (R)-enantiomer of BABA to aspartyl-tRNA synthetase (AspRS) (Luna et al., 2014a). BABA has shown efficacy in several crops, including the model plant A. thaliana (Koen et al., 2014; van Hulten et al., 2006; Zimmerli et al., 2001) and tomato (Koen et al., 2014; Luna et al., 2016, 2020; van Hulten et al., 2006; Wilkinson et al., 2017; Zimmerli et al., 2001) as well as in postharvest protection of grapevine (Csikász-Krizsics et al., 2013), onions (Polyakovskii et al., 2008), and strawberries (Wang et al., 2016). Its effect on the strawberry plant is highly variable, from enhanced resistance to increased susceptibility, depending on application method, BABA concentrations, and plant developmental stage (Badmi et al., 2022, 2019).

Despite its potential, BABA application for crop protection has been hampered by its growth-inhibiting properties, which result from the inhibitory binding of BABA to AspRS enzymes, thereby competing with Asp and preventing its binding (Luna et al., 2014a). However, while some studies reported remarkable effects on growth and yield (Badmi et al., 2019; Buswell et al., 2018; van Hulten et al., 2006), others report just a transient growth reduction (Luna et al., 2014b; Wilkinson et al., 2017) or no effects (Badmi et al., 2019), highlighting the importance of species-specific evaluation. To overcome these drawbacks, BABA analogues, such as (R)-βhomoserine (RBH), have been investigated against B. cinerea. RBH retains IR-inducing properties without causing growth suppression and has been shown to prime JA defences in tomato and to provide long-lasting protection in Fragaria vesca plants (Badmi et al., 2019; Buswell et al., 2018). Another candidate priming agent is indole-3-carboxylic acid (I3CA), a metabolite that has been found to accumulate in BABA-primed A. thaliana upon infection with Plectosphaerella cucumerina (Gamir et al., 2012, 2014). When exogenously applied, I3CA was effective in inducing resistance against P. cucumerina, but the I3CA-IR appeared to be independent of the SA and JA pathways (Gamir et al., 2014). Moreover, no study has been conducted to assess its effects on plant growth. Therefore, further studies are needed to understand the mechanisms underlying I3CA-induced resistance against necrotrophic pathogens and evaluate its suitability for crop protection. BABA, RBH, and I3CA showed no direct antifungal

activity, supporting the idea that their efficacy is plant-mediated rather than due to directly killing the pathogen (Badmi et al., 2019; Buswell et al., 2018; Gamir et al., 2014). However, their efficacy in strawberry, as well as the underlying mechanisms, remains underexplored. Priming induced by elicitor application presents a sustainable and promising strategy for protecting crops from *B. cinerea*. Since priming involves complex biochemical changes, metabolomic approaches provide a powerful tool for unravelling the complex mechanisms behind defence priming. Identifying key metabolic pathways and markers associated with IR could facilitate the development of more sustainable chemical strategies. To date, a comprehensive metabolomic analysis to unravel IR mechanisms primed by SA, JA, BABA, RBH, and I3CA in strawberry against *B. cinerea* is lacking.

No fully resistant genotypes have been identified, and the genetic and biochemical factors contributing to resistance against *B. cinerea* remain largely unknown (Bestfleisch et al., 2015). For instance, the resistance of strawberry against *B. cinerea* is described as quantitative disease resistance (QDR), which leads to partial resistance, and its success may be highly affected by external factors, such as environment, plant species and variety, and plant developmental stages. On the other hand, the high pathogenicity of *B. cinerea* in strawberry arises from the ability to deploy a rich toolbox of nonspecific pathogenicity factors for which no known resistance (R) genes in strawberry are available (Bi et al., 2023). Moreover, non-genetic variables in field studies (*e.g.*, row density, climatic conditions) have been considered as the primary cause of slight differential susceptibility (Rhainds et al., 2002).

Thus, this study investigates: (1) the efficacy of BABA, RBH, I3CA, JA, and SA in inducing resistance to *B. cinerea* in three commercial strawberry cultivars (Durban, Rowena, and Soraya); (2) the mechanisms of IR through untargeted metabolomics; (3) the metabolic pathways and key metabolites involved in priming; and (4) the potential growth reduction and fitness costs of elicitor treatments. Our results aim to provide novel insights into the defence responses of strawberries to *B. cinerea* and the mechanisms of defence priming agents, thereby developing new sustainable crop protection strategies.

Materials and methods

Plant material and growth conditions

Plants of three *Fragaria* × *ananassa* cultivars, Durban, Rowena, and Soraya, were obtained from achenes (ABZ seeds, UK, kindly provided by Saturn Bioponics https://saturnbioponics.com/). Achenes were germinated on wetted filter paper in sealed Petri dishes under long-day conditions (16 h light/8 h dark, 25 °C/20 °C, 100% relative humidity) in a growth chamber. After two weeks, uniformly germinated seedlings were transplanted into alveolar trays (80 mL volume per cell) filled with Levington M3 compost (catalogue number: PHSM-1-1-1-1). Plants were grown under the same photoperiod, temperatures, and light intensity until they reached 18 weeks of age. Water and nutrient supply were

adjusted according to plant phenological stages using the commercial fertigation protocols of Vitax Organic Strawberry Fertiliser (Catalogue number 5LSF1).

Pathogen culture and inoculum preparation

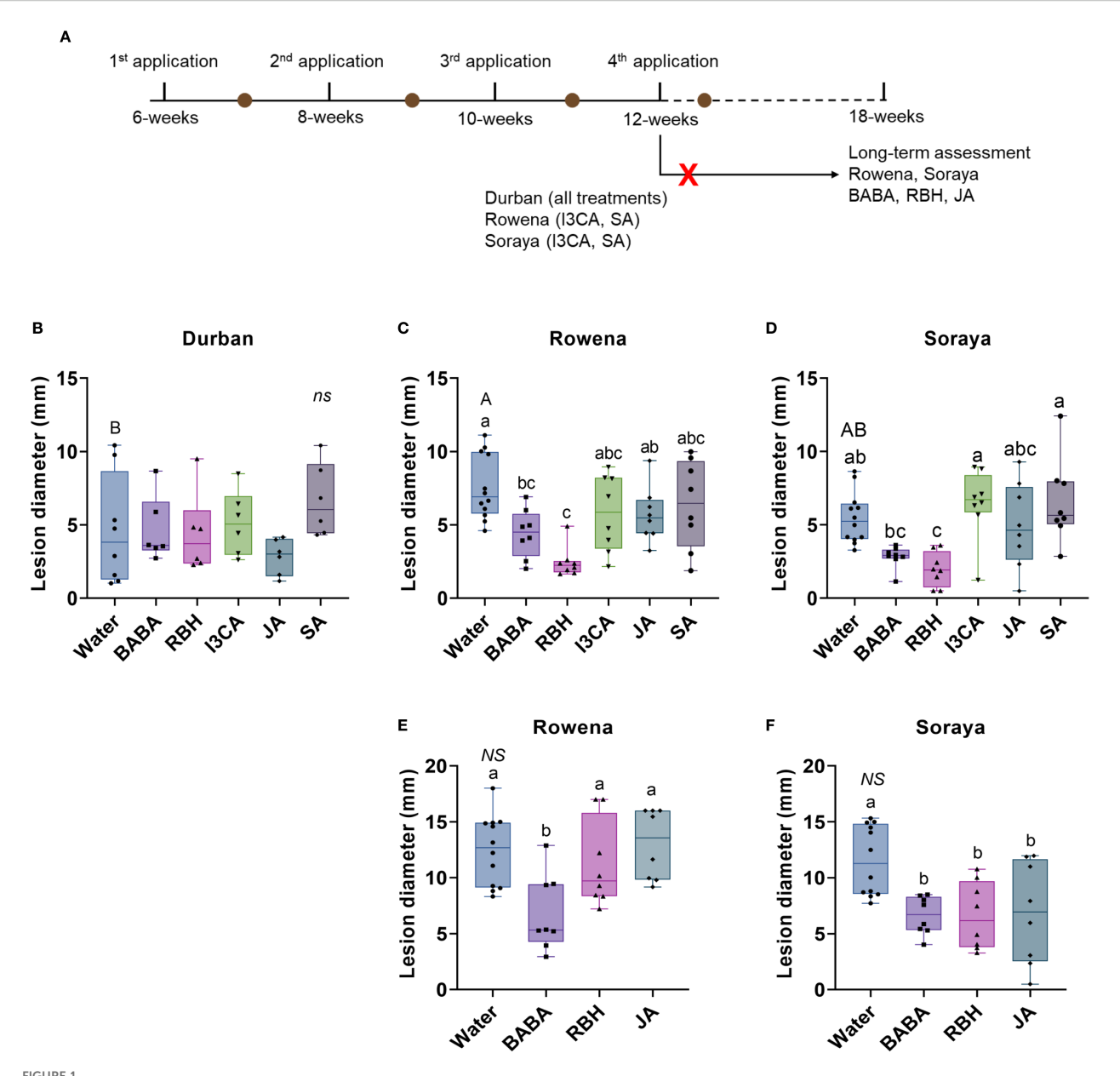
Botrytis cinerea isolate BcI16 (Faretra and Pollastro, 1991) was cultured on potato dextrose agar (PDA) plates. A single agar plug from a sporulated colony was transferred to fresh PDA and incubated in the dark at room temperature for four weeks as previously described (Stevens et al., 2025). Spores were collected in sterile water containing 0.01% Tween-20, filtered through Miracloth (EDM Millipore, Burlington, MA, USA), and pelleted by centrifugation (10 min at 4,000 rpm). The final spore concentration of the inoculum was adjusted to 5×10^5 spores/mL in half-strength potato dextrose broth (PDB).

Elicitor treatments

Five elicitors were tested: β-aminobutyric acid (BABA), (R)-βhomoserine (RBH), indole-3-carboxylic acid (I3CA), jasmonic acid (JA), and salicylic acid (SA). Compounds were obtained from Sigma-Aldrich and prepared freshly prior to application. BABA and RBH were applied at 0.5 mM, I3CA at 0.150 µM, JA at 0.1 mM, and SA at 1 mM final concentrations. BABA, RBH, and I3CA were applied via soil drenching by injecting a 10x concentrated solution at 10% of the tray's alveolus volume (80 mL). BABA and RBH were dissolved in sterile distilled water (SDW). I3CA was dissolved in ethanol and then diluted to the selected concentration. The final ethanol concentration in the solution was 0.075%, and therefore, all soil drench solutions were supplemented with ethanol to achieve this concentration. JA and SA were applied as foliar sprays until runoff on both adaxial and abaxial leaf surfaces. SA was dissolved in SDW. Stock solutions of JA were prepared according to Luna et al. (2016) by dissolving 250 mg in 2 ml of ethanol, then diluted in distilled water to a final stock concentration of 10 mM, and stored at -20 °C. Before use, the 10 mM stock solution was thawed and diluted to the final concentration in the spraying solution, resulting in a final ethanol concentration of 0.042%. Therefore, all other spraying solutions were supplemented with 0.042% ethanol. All foliar spray solutions contained 0.01% Silwet to improve adherence to leaf surfaces. Solvent solutions only (without chemicals) were used to treat control plants (i.e., Water treatment), and the soil-drench solution and spraying solution were applied to each treatment to equalise the amount of solvent in the soil or on the leaves. All treatments were applied four times at 2-week intervals on plants aged 6, 8, 10, and 12 weeks (Figure 1A).

Leaf infection assay with B. cinerea

Detached leaf assays were conducted five days after each treatment application. One fully expanded leaf (trifoliate) was



Induced resistance to *B. cinerea* in strawberry cultivars treated with chemical elicitors. (A) Experimental timeline showing four elicitor applications at 6, 8, 10, 12, and 18 weeks of plant age and subsequent leaf inoculations with *B. cinerea* for disease assessment. The brown dots indicate leaf inoculations performed five days after the application of the elicitors. The red cross indicates the treatments that were excluded from the long-term assessment. Lesion diameter in Durban (B), Rowena (C), and Soraya (D) after four elicitor applications. Lesion diameter six weeks after the final elicitor application (18-week-old plants) in Rowena (E) and Soraya (F). Boxplots represent lesion diameter (mm) with the median line, interquartile range (boxes), and whiskers extending to the minimum and maximum values. Each point represents biological replicates (individual plants) (n = 8–12) per treatment). Capital letters indicate statistical differences between the Water treatments of each variety. Lowercase letters indicate statistically significant differences between elicitors within each variety (One-way ANOVA followed by Tukey's *post hoc* test or Welch's ANOVA followed by Dunnett's T3; p < 0.05; n = 8-12) NS indicates not significant.

selected for infection in each plant. Detached leaves (n = 8-12) were infected by applying 5 μ L of the drop inoculum solution on either side of the main vein (*i.e.*, 2 drops/foliole). Mock leaves were infected with ½ strength PDB only. Inoculated leaves were incubated at 20 °C in the dark at 100% RH. Disease incidence was measured as necrotic lesion diameter (mm) five days post-inoculation using an electronic calliper (0.1 mm resolution).

Growth and reproductive performance assessment

Relative growth rate (RGR) for leaf area was calculated between the time points one week before the fourth elicitor application (t1; week 11 of the experiment) and two weeks after the same application (t2; week 14 of the experiment). The following

formula was used: $RGR = [ln(leaf area_{t2}) - ln(leaf area_{t1})]/(t_2 - t_1)$. Leaf area was measured with ImageJ Software [Version 1.54j, https://imagej.net/ (Schneider et al., 2012)]. Flowering was recorded on 11- and 13-week-old plants, while fruit production was assessed on 18-week-old plants (six weeks after the fourth application), by counting the number of flowers and fruits per treatment.

Statistical analysis

Data normality was assessed using the Shapiro-Wilk test (p \geq 0.05). Homogeneity of variance was evaluated with Levene's test. For normally distributed data with equal variances, one-way ANOVA followed by Tukey's post hoc test was used. When variances were unequal, Welch's ANOVA followed by Dunnett's T3 test was applied. Analyses were performed in GraphPad Prism 9 (GraphPad Software, San Diego, CA, USA).

Metabolomic analysis

Sample collection for metabolomic analysis

For metabolomic analysis, leaves were collected from individual plants (n = 8-12) of Rowena and Soraya, following treatment with Water, BABA, RBH, and JA 5 days after the final application. Infected and mock-infected leaves were collected 24 hours post-infection (hpi), snap-frozen in liquid nitrogen, ground in liquid nitrogen, and lyophilized before metabolite extraction. For each condition, three biological replicates were used. Each biological replicate consisted of a pool of one leaf per plant, using four plants for the Water treatments and two to three plants for the chemical treatments.

Metabolite extraction and LC-QTOF analysis

Three biological replicates and three techniques were used for the analysis (n = 6). The metabolites were extracted using a mixture of MeOH and H₂O (30:70) supplemented with 0.01% HCOOH. Then, 1 mL of 30% MeOH was added to 300 mg of powdered freeze-dried tissue, and the samples were incubated on ice for 30 min. After shaking for 15 min and centrifugation at 15.000 rpm for 15 min at 4 °C, the supernatant was filtered using a 0.2 μm cellulose filter. An aliquot (5 µL) of each sample was injected into the hybrid tandem UPLC-QTOF (Synapt, Waters) mass spectrometer in the positive (ESI +) and negative (ESI -) ion modes for electrospray ionization. Samples elution was performed through a reversedphase C-18 column (Kinetex EVO C18 Core-Shell, 2.6 µm particle size, Phenomenex) with a gradient of MeOH and H2O supplemented with 0.01% HCOOH. Raw data can be found in Metabolights (ID: MTBLS12834, https://www.ebi.ac.uk/ metabolights/MTBLS12834).

Raw data were transformed into. mzML format using the MSConvert tool from ProteoWizard (Chambers et al., 2012). Data were processed using R software [version 4.4.1 (R Core Team,

2024)] where ESI+ and ESI- signals were analysed separately. Signal corrections were obtained using the Centwave algorithm for R. The amount of each compound was determined from the normalized peak area relative to the dry weight of each sample.

Global data visualization and statistical analysis

Global visualization of the combined ESI+ and ESI- data was performed using Principal Component Analysis (PCA) and a heatmap in Metaboanalyst 6.0 (Pang et al., 2024), applying filtering through the interquartile range (<40%), normalization by median, followed by cube root transformation and Pareto scaling for combined positive and negative ionization mode data. For PCA, statistical significance between the treatment groups was evaluated using PERMANOVA (p ≤ 0.05). Heatmaps were obtained using hierarchical clustering, Euclidean distance measurement, and Ward's clustering method, and metabolite expression was represented as group averages. A log₂ fold change measure was used to determine up- or down-expression levels of metabolites. Venn diagrams were drawn using Venny [version 2.1.0 (Oliveros, 2007-2015)], and the significant putative metabolites associated with each treatment and infection condition were determined using a two-sample t-test (FDR, $p \le 0.05$) between the elicitor and Water treatments under both mock and B. cinerea infection.

Pathway enrichment analysis of priming metabolites

Priming metabolites were isolated from Venn diagrams by comparing the elicitor vs. Water upon mock infection and the elicitor vs. Water upon pathogen infection and selecting significant metabolites solely associated with infection. These metabolites were putatively identified through several metabolite libraries, one available in the KEGG database for Fragaria vesca and one internal library kindly provided by Dr. Pastor's group, created using pure chemical standards to record the specific retention time, exact mass, and spectrum fragmentation, as described in Gamir et al. (2014). The priming metabolites specific to each compound underwent enrichment pathway analysis using the MarVis-Suite software [version 2.0, https://marvis.gobics.de/ (Kaever et al., 2015, 2009)]. Adduct and isotope correction, followed by merging of the positive and negative ionization mode data, was performed using the MarVis-Filter, while the pathways were obtained from the MarVis-Pathway. Entry-based enrichment analysis calculated p-values based on a hypergeometric distribution, which were then adjusted using FDR (Benjamini-Hochberg) correction. Pathways with p-values ≤0.05 were considered significantly enriched. The putatively annotated Metabolites of enriched pathways were further identified at a confidence level (MS1 MS2) in MassLynx (version 4.2, Waters Corporation, https:// www.waters.com/) through ChromaLynx. When fragmentation spectra were not available in the selected libraries, fragmentation spectra from online databases of PubChem (https:// pubchem.ncbi.nlm.nih.gov/), and Human Metabolome Database (HMDB, https://www.hmdb.ca/) were considered, with similar LC-MS/MS experimental conditions and ionization modes.

Results

Efficacy of elicitors in inducing resistance to *B. cinerea*

To evaluate the ability of five chemical elicitors (*i.e.*, BABA, RBH, I3CA, JA, and SA) to induce resistance against *B. cinerea*, four applications were carried out at two-week intervals on strawberry cultivars Durban, Rowena, and Soraya at 6, 8, 10, and 12 weeks of age (Figure 1A). A leaf infection assay was carried out five days after the application of the elicitors. Following inoculation, disease incidence was measured as lesion diameter (mm) five days post-infection.

Before elicitor analysis, basal resistance levels among the three cultivars were first assessed for Water-treated controls. No significant differences were observed after the first application (Supplementary Figure 1A). However, after the second application, Rowena exhibited higher susceptibility than Soraya, while Durban showed an intermediate response (Supplementary Figure 1B). These differences were not observed after the third application (Supplementary Figure 1C). However, after four applications, Rowena exhibited significantly higher susceptibility compared to Durban, indicating the lowest basal resistance at the 12-week-old stage, while Soraya showed intermediate lesion sizes compared to Durban and Rowena (Figures 1B-D).

IR was analysed after each elicitor application. A single treatment was insufficient to induce resistance in any of the cultivars (Supplementary Figure 1A). However, from the second application, resistance began to emerge in some treatments. In Durban, JA significantly reduced lesion size by 72.5% and 88.4% after the second and third applications, respectively (Supplementary Figures 1B, C). This effect was not sustained after the fourth application (Figure 1B), where none of the elicitors reduced lesion size in Durban. In contrast, in Rowena and Soraya, none of the elicitors induced statistically significant reductions in lesion size until the fourth application (Supplementary Figures 1A-C; Figures 1C, D). After the fourth application, whereas JA, SA, and I3CA did not induce resistance in Rowena, BABA treatment reduced lesion size by 41.6% compared to the Water control (Figure 1C). RBH was even more effective, reducing lesion size by 67.5% compared to Water (Figure 1C). In Soraya, RBH also significantly reduced lesion size by 64% after four applications (Figure 1D). However, none of the other elicitors, including BABA, result in a statistically significant difference in lesion size (Figure 1D).

To test the durability of these effects, additional assays were conducted on 18-week-old plants, six weeks after the final elicitor application. Differences in basal resistance between Rowena and Soraya at this developmental stage were not found (Figures 1E, F). In Rowena, BABA was the only elicitor to result in a reduced lesion size (45.3% compared to the control) (Figure 1E). In Soraya, RBH maintained a 42.6% reduction (Figure 1F). Interestingly, BABA and JA treatments also reduced lesion sizes by 44.8% and 40.7%, respectively (Figure 1F). These findings indicate that BABA, RBH, and JA can induce long-lasting resistance effects in specific cultivars.

Relative growth rate analysis, flowering, and fruit production assessment

To evaluate whether repeated elicitor treatments impacted strawberry development, we assessed plant growth and reproductive traits following four consecutive applications from the seedling to the mature stage. RGR was calculated from nondestructive leaf area measurements between weeks 11 and 14. No significant differences (p > 0.05) in RGR were observed across treatments in any of the three cultivars (Supplementary Figure 2). This approach enabled the tracking of individual plant growth over time, thereby avoiding the need for destructive harvesting and allowing for the subsequent assessment of flowering and fruiting. Flowering was recorded on 11- and 13-week-old plants, while fruit production was assessed on 18-week-old plants (six weeks after the fourth application), by counting the number of flowers and fruits per treatment. No statistically significant differences in inhibition of flower (Supplementary Table 1) or fruit (Supplementary Table 2) production were found in any cultivar. While flower numbers were generally higher than fruit numbers, this reduction was observed across all treatments, including Water controls, indicating poor flower-to-fruit conversion irrespective of elicitor application. Although some differences in mean flower and fruit numbers were observed between treatments, variability between individual plants was high, and these differences were not statistically significant (Supplementary Tables 1, 2).

Metabolomic profiling of elicitor-induced resistance

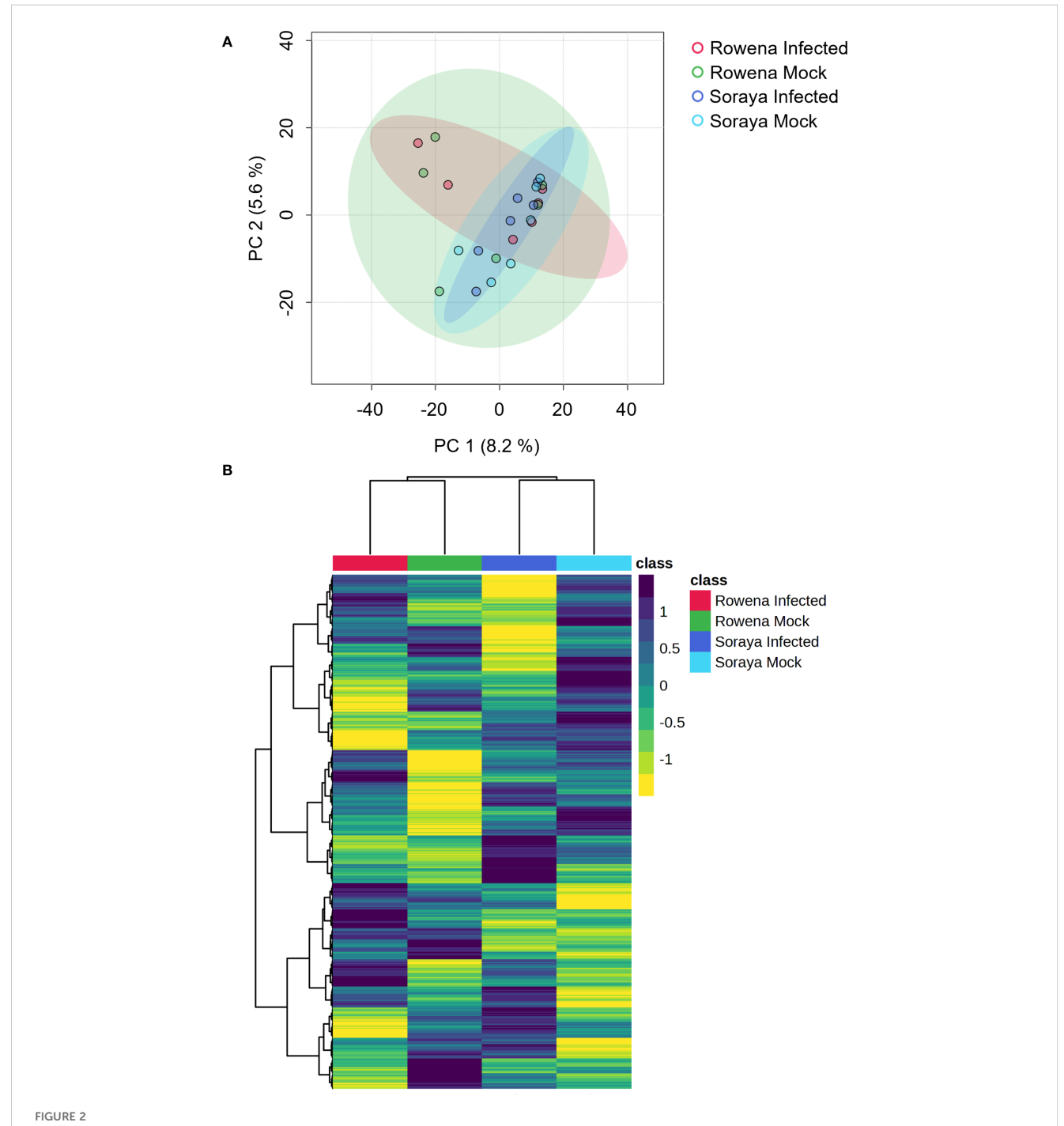
To investigate the underlying mechanisms of induced resistance, an untargeted metabolomic analysis was conducted in Rowena and Soraya treated with Water, BABA, RBH, and JA, and then challenged with *B. cinerea* or a mock treatment. A total of 14,603 metabolomic features were detected, including 9,647 under positive electrospray ionization (ESI+) and 4,956 under negative mode (ESI-).

Variety-specific metabolomic profiles to infection

First, to investigate whether differences in basal resistance between cultivars could be associated with distinct constitutive metabolic profiles, we performed a PCA and hierarchical clustering heatmap analysis on mock- and *B. cinerea*-infected Water-treated plants (Figure 2). This was done to mirror the assessment shown in Figures 1C,D, where cultivar-specific differences in lesion size were observed. Figure 2A shows a PCA based on metabolomic features of Rowena and Soraya in the absence and presence of *B. cinerea*. The first two principal components (PC) explained 13.8% of the total variability, with the first component (PC1) accounting for 8,2% and the second component (PC2) accounting for 5.6%. While *B. cinerea* infection

alone did not significantly alter the global metabolome at 24 hpi (PERMANOVA, F = 0.28, $R^2 = 0.04$, p = 0.942), orientation along PC1 reflects underlying metabolic differences between the two cultivars. The heatmap revealed a strong separation between Rowena and Soraya, with mock and infected samples clustered

closely within each cultivar (Figure 2B). This supports the PCA results and confirms that infection had minimal impact on the global metabolic profile at 24 hpi, and that constitutive metabolomic differences exist between cultivars with contrasting basal resistance.



Basal metabolomic differences between strawberry cultivars with contrasting susceptibility to *B. cinerea*. (A) Principal Component Analysis (PCA) of metabolomic profiles in Water-treated Rowena and Soraya plants under mock- and *B. cinerea*-inoculated conditions. Samples were collected 24 hours post-inoculation. Each point in the PCA represents one replicate (n = six per condition; three biological replicates; two technical replicates). PERMANOVA was used to assess statistical significance. Ellipses represent the 95% confidence intervals for each treatment group means.

(B) Hierarchical clustering heatmap of metabolomic features from the same samples.

Metabolomic impact of BABA, RBH, and JA in Rowena and Soraya

Next, we assessed whether elicitor treatments triggered changes in the metabolic profiles of each cultivar and whether these changes were influenced by B. cinerea infection. While the PCA plots displayed relatively low explanatory variance on the first two components, this is a common feature in untargeted metabolomics datasets where high dimensionality and biological variability can limit the percentage of explained variance. Despite this, the observed separations were statistically supported by PERMANOVA analyses, indicating that the metabolic profiles among treatments and cultivars were significantly different and biologically meaningful. In the PCA of Rowena samples under mock conditions, the first two PCs explained 24.5% of the total variability, with PC1 accounting for 13.6% and PC2 accounting for 10.9%. This PCA revealed clear separation between treatment groups (PERMANOVA, F = 5.66, $R^2 = 0.45$, p = 0.001; Figure 3A), with RBH showing the most distinct profile compared to Water, JA, and BABA. Under B. cinerea infection, PCs explained 28.9% of the total variability, with PC1 accounting for 17.9% and PC2 accounting for 11%. Again, it showed a significant treatment effect (PERMANOVA, F = 5.37, R² = 0.44, p = 0.001; Figure 3B). Notably, RBH remained the most metabolically distinct, while BABA showed a more evident divergence from Water upon infection than in the mock conditions.

In the PCA of Soraya samples under mock conditions, PCs explained 25.7% of the total variability, with PC1 accounting for 15.9% and PC2 accounting for 9.8%. Upon *B. cinerea* infection, PCs explained 27.1% of the total variability, with PC1 accounting for 15.8% and PC2 accounting for 11.3%. Similarly to the previous case, in Soraya, PCA also revealed significant treatment effects under both mock (PERMANOVA, F = 2.71, $R^2 = 0.29$, p = 0.027; Figure 3C) and infected conditions (PERMANOVA, F = 3.20, $R^2 = 0.32$, p = 0.012; Figure 3D). BABA had the most substantial impact, significantly altering the metabolome compared to Water and RBH in mock conditions and to Water under infection. These results suggest that elicitor-induced metabolic changes vary depending on both the cultivar and the presence of *B. cinerea*, with RBH being most effective in Rowena and BABA in Soraya.

A global view of elicitor-induced metabolic changes was further assessed through hierarchical clustering heatmap analysis, where the metabolic features detected in both ESI+ and ESI- modes were grouped according to treatment and compared between mock- and *B. cinerea*-inoculated conditions (Figures 3E, F).

In Rowena, clustering analysis revealed six significant metabolite clusters with expression patterns across treatments and infection conditions (Figure 3E). Cluster 1 included metabolites upregulated by RBH under mock conditions, downregulated by infection in Water-treated plants, and subsequently upregulated again in both BABA- and RBH-infected samples. Cluster 2 consisted of metabolites consistently upregulated by BABA under both mock and infected conditions. Cluster 3 showed metabolites upregulated by JA in both mock and infected samples, downregulated by RBH following infection (i.e., priming of RBH

cluster), and an upregulated by BABA upon infection (*i.e.*, priming of BABA cluster). Cluster 4 was defined by metabolites that were specifically upregulated after RBH treatment and infection (*i.e.*, priming of the RBH cluster). Cluster 5 includes metabolites downregulated by RBH under both mock and infected conditions, with a greater impact of the infection (*i.e.*, priming of RBH cluster). Cluster 6 represented metabolites that were consistently downregulated by all three elicitor treatments, regardless of the infection status.

In Soraya, six distinct clusters were identified (Figure 3F). Cluster 1 included metabolites with different profiles upon treatments and infection. Cluster 2 was associated with metabolites downregulated in BABA treatment and, to a much greater extent, in BABA-infected samples (*i.e.*, priming of the BABA cluster). Cluster 3 was defined by downregulation of metabolites after BABA treatment and infection (*i.e.*, priming of the BABA cluster). Cluster 4 contained features downregulated in the BABA mock and upregulated in the JA mock. Cluster 5 captured metabolites that were upregulated under BABA mock conditions and to a much greater extent in BABA-infected samples (*i.e.*, priming of the BABA cluster). Finally, Cluster 6 grouped features that were upregulated in BABA mock, downregulated in Water-infected plants, and upregulated in JA upon infection (*i.e.*, priming of the JA cluster).

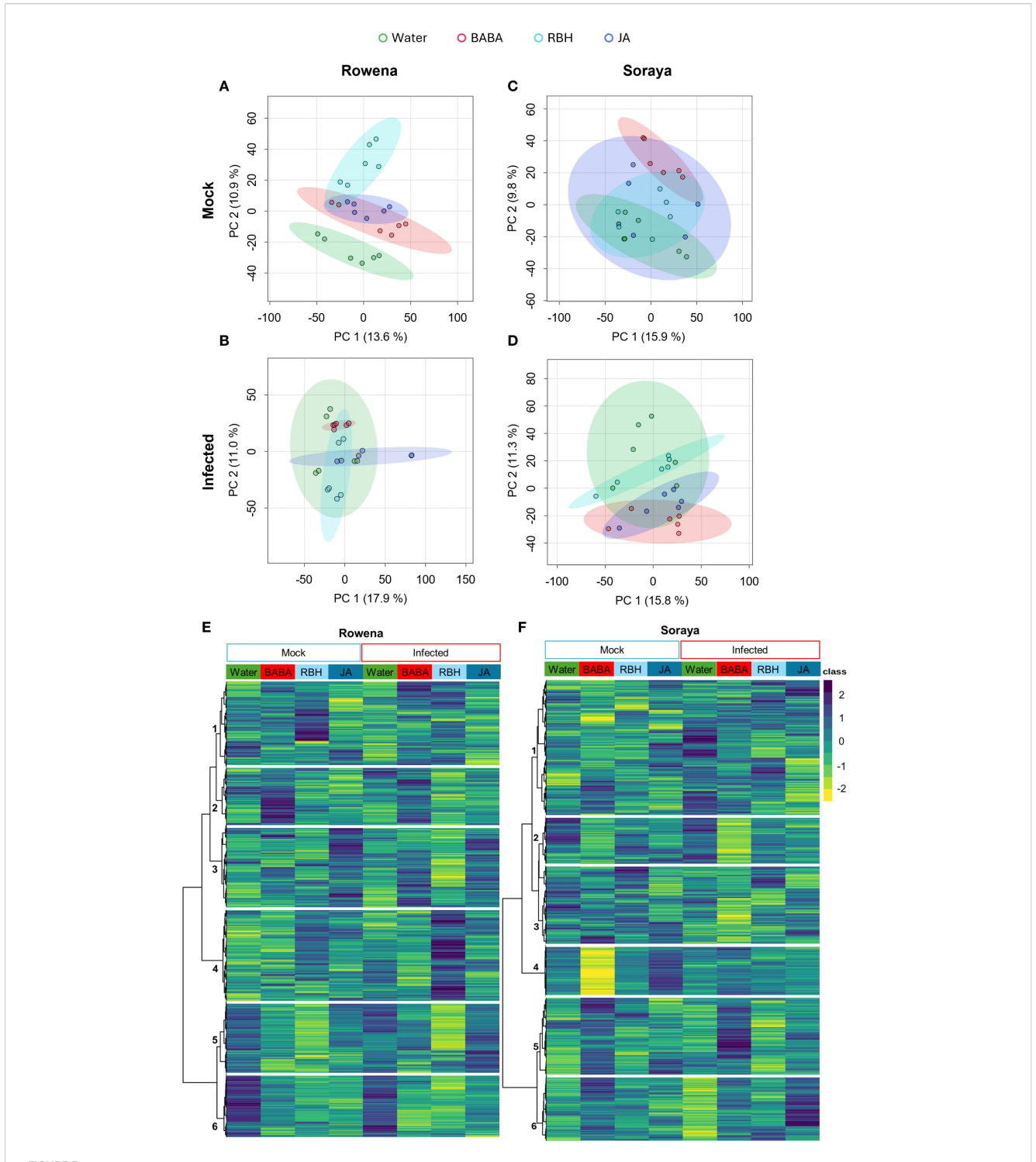
Isolation of direct and priming compounds and primed pathways identification in Rowena

To identify metabolites specifically associated with elicitor-induced resistance, we performed pairwise comparisons between each elicitor treatment and the Water control under both mockand *B. cinerea*-inoculated conditions. Significant metabolites unique to either condition were categorised as "direct" (mock only) or "priming" (infection only).

In Rowena, when comparing all the putative metabolites under mock conditions, we observed that RBH triggered the most substantial metabolic reprogramming, with 348 (41.7%) induced metabolites, followed by JA (222, 26.6%) and BABA (32, 3.8%) (Supplementary Figure 3A). Shared metabolite changes included 64 between the three elicitors, 124 between RBH and JA, 27 between RBH and BABA, and 17 between JA and BABA. Upon *B. cinerea* infection, RBH continued to dominate the metabolic response, inducing 357 (58.8%) metabolites, followed by BABA (136, 22.4%) and JA (7, 1.2%) (Supplementary Figure 3B). Infected samples had no shared metabolites between the three elicitors, and only 107 were shared between BABA and RBH.

To isolate direct activators (elicitor-induced under mock conditions only), Venn diagrams between mock and infected for each elicitor showed 425 JA-, 339 RBH-, and 82 BABA-associated metabolites (Supplementary Figure 3C). These were further grouped to identify metabolites uniquely associated with each elicitor (Figure 4A). After this filtering (where the impact of the infection was removed), the effect of JA on the metabolome was

10.3389/fpls.2025.1675649 Murena et al.



Metabolomic shifts in strawberry cultivars following elicitor treatments under mock and B. cinerea-inoculated conditions. Principal Component Analysis (PCA) of metabolic profiles in Rowena (A) and Soraya (C) under mock conditions and in Rowena (B) and Soraya (D) under B. cinerea infection. Samples were collected 24 hours post-inoculation. Each point represents one biological replicate (n = six per condition; three biological replicates; two technical replicates). Significant separation of treatment groups was observed by PERMANOVA (p < 0.05). Ellipses represent the 95%confidence intervals for each treatment group means. (E) Hierarchical clustering heatmap of metabolomic features in Rowena across treatments (Water, BABA, RBH, and JA) under both mock and infected conditions. (F) Hierarchical clustering heatmap of metabolomic features in Soraya across the same treatments and conditions. Clusters highlight treatment- and cultivar-specific metabolic reprogramming.

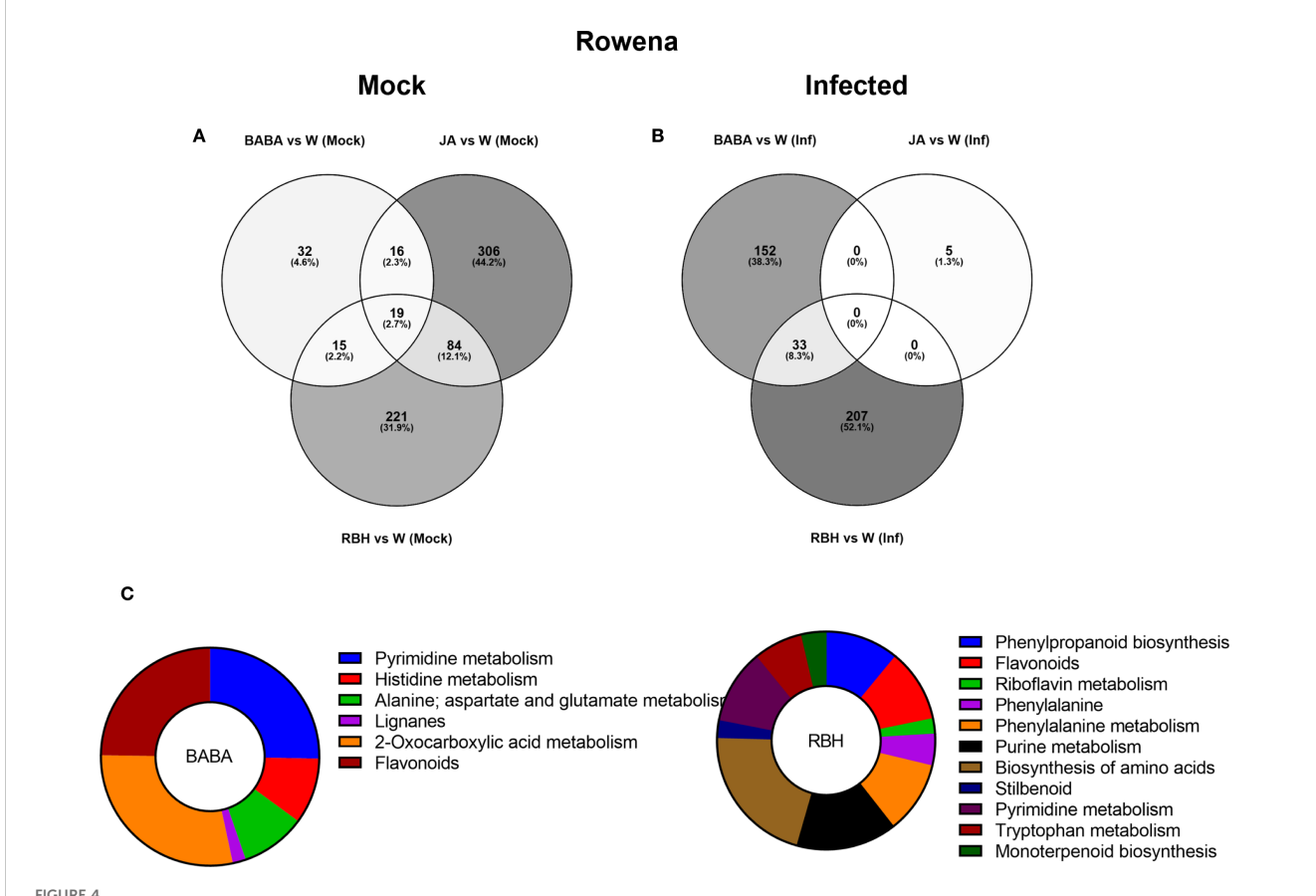
more pronounced than the previously observed effect of RBH, with 306 (44.2%) metabolites being induced, followed by 221 (31.9%) RBH-induced and 32 (4.6%) BABA-induced (Figure 4A).

Priming-associated metabolites (elicitor-induced only upon *B. cinerea* infection) were also identified. Similar filtering was done to isolate metabolites associated only with the infection, which resulted in 240 RBH-specific, followed by 185 BABA- and 5 JA-associated features (Supplementary Figure 3C). After this filtering (where the impact of the direct effect of the elicitor was removed), we observed that 207 (52.1%) were exclusive to RBH, 152 (38.3%) to BABA, and 5 (1.3%) to JA. Only a shared group of 33 (8.3%) metabolites was found between BABA and RBH (Figure 4B).

Priming-associated metabolites from Rowena were selected based on their unique association with BABA, RBH, or JA treatments, as identified in the Venn diagrams. These metabolites were subjected to putative annotation by comparison with two reference libraries: the KEGG database for *Fragaria vesca* and an internal library kindly provided by Dr. Pastor's group. Metabolite identifications were made in MassLynx using ChromaLynx, with confidence levels based on retention time and spectral matching

(MS level). Where fragmentation spectra were not available in the selected libraries, complementary spectra were retrieved from public databases (e.g., PubChem, HMDB) using similar LC-MS/MS experimental parameters and ionization modes.

A total of 62 metabolites were putatively identified in Rowena: 23 were uniquely associated with BABA, 37 with RBH, and 2 were common to both treatments (Table 1). Enrichment analysis revealed statistically significant metabolic pathways related to these priming responses for BABA and RBH only. For BABA, enriched pathways included Alanine metabolism (3 metabolite; 2 up, 1 up), Flavonoids (5 metabolites, all down), Histidine metabolism (5 metabolites; 4 up, 1 down), Lignans (1 metabolite, up), Pyrimidine metabolism (4 metabolites; 3 up, 1 down), and 2-Oxocarboxylic acid metabolism (5 metabolites: 4 up, 1 down) (Figure 4C). RBH-associated priming metabolites were significantly enriched in Biosynthesis of amino acids (2 metabolites, down), Flavonoids (7 metabolites; 6 down, 1 up), Monoterpenoid biosynthesis (1 metabolite up), Phenylalaninetyrosine-tryptophan biosynthesis (2 metabolites, 1 up, 1 down), Phenylalanine metabolism (4 metabolites; 3 down, 1 up),



Metabolomic responses to elicitor treatments in Rowena. (A) Venn diagram showing the number of metabolites exclusively induced under mock conditions (no infection) by RBH, BABA, and JA in Rowena. (B) Venn diagram showing the number of metabolites exclusively induced under B. cinerea infected conditions by RBH, BABA, or JA in Rowena. Percentages represent each elicitor's contribution to the total number of direct/priming-associated features. The number of shared metabolites between treatments is also indicated. (C) Pathway enrichment of priming-associated metabolites in Rowena. Putatively annotated priming-associated metabolites uniquely induced by BABA and RBH in B. cinerea-infected Rowena plants were subjected to pathway enrichment analysis using the KEGG database for Fragaria vesca and one internal library. Pie charts represent the percentage of statistically significant enriched pathways (p < 0.05) for BABA (left) and RBH (right), based on the number of annotated metabolites per pathway, are shown for each elicitor.

Murena et al.

TABLE 1 Summary of the pathways enriched by BABA, RBH and JA treatment in Rowena and the identified metabolites associated to those pathways.

Pathway	Putative compound	Predicted formula	Adduct	Parental ion	Fragments	BABA	RBH	JA
Alanine; aspartate and glutamate metabolism	2-Ketoglutaric acid	$C_5H_6O_5$	[M-H]	145.0290	72.70>78.600	Up	-	-
	Fumaric acid	$C_4H_4O_4$	[M+H] ⁺	117.0180	55.0183>71.013>73.029	Down	-	_
	N-Acetyl-L-aspartic acid	C ₆ H ₉ NO ₂	[M-H] ⁻	174.0119	58.0298>114.018>88.039	Up	-	-
Biosynthesis of amino acids	Carbamoyl phosphate	CH ₄ NO ₅ P	[M-H]	140.0065	78,959	-	Down	_
	(3-Indolyl)-glycerol phosphate	C ₁₁ H ₁₄ NO ₆ P	[M+H] ⁺	288.0849	80.9736>118.0651>146.060	-	Down	_
Flavonoids	5;7-Dihydroxychromone	C ₉ H ₆ O ₄	[M-H] ⁻	177.0552	133,029	Down	Down	_
	Luteolin	$C_{15}H_{10}O_{6}$	[M-H]	285.0403	109.028>133.028>223.007	-	Down	_
	Tectorigenin	$C_{16}H_{12}O_{6}$	[M-H]	299.0192	183.0121>284.0322	-	Up	-
	Avicularin	$C_{20}H_{18}O_{11}$	[M+H] ⁺	435.0569	255.0296>271.0258>300.0268	-	Down	-
	Sec-O-Glucosylhamaudol	$C_{21}H_{26}O_{10}$	[M-H]	437.1000	91.0544>149.060>201.046	-	Down	-
	Astilbin	$C_{21}H_{22}O_{11}$	[M-H]	449.1093	151.0028>271.039>285.039	-	Down	-
	Isoquercitrin	$C_{21}H_{20}O_{12}$	[M-H]-	463.0775	284.0318<301.0701	Down	Down	-
	4-Hydroxychalcone	C ₁₅ H ₁₂ O ₂	[M+H] ⁺	225.1117	83.049>183.0113>205.0643	Down	-	-
	Cimifugin	C ₁₆ H ₁₈ O ₆	[M+H] ⁺	307.1154	221.045>235.060>259.061	Down	-	-
	Homoplantaginin	C ₂₂ H ₂₂ O ₁₁	[M-H]	461.1084	119.0495>269.0444>283.0243	Down	-	-
Histidine metabolism	Imidazole acetaldehyde	C ₅ H ₆ N ₂ O	[M+H] ⁺	111.0446	42.033>56.049>66.033>81.0447	Up	-	-
	Imidazole-4-acetate	$C_5H_6N_2O_2$	[M-H]	125.0240	71.631>81.044	Down	-	-
	2-Ketoglutaric acid	C ₅ H ₆ O ₅	[M-H]	145.0290	72.70>78.600	Up	-	-
	4;5-Dihydro-4-oxo-5- imidazolepropanoate	$C_6H_8N_2O_3$	[M-H] ⁻	154.9982	41.999>59.013>81.00094	Up	-	-
	N-Formyl-L-glutamate	C ₆ H ₉ NO ₅	[M-H]	174.0120	41.998>44.0142>102.056	Up	-	-
Lignanes	Deoxypodophyllotoxin	C ₂₂ H ₂₂ O ₇	[M+H] ⁺	399.1244	399,1467	Up	-	-
Monoterpenoid metabolism	6-endo-Hydroxycineole	C ₁₀ H ₁₈ O ₂	[M+H] ⁺	171.1502	153,127>171,138	-	Up	-
2-Oxocarboxylic acid metabolism	2-Keto-3-methylbutyric acid	C ₅ H ₈ O ₃	[M+H] ⁺	117.0187	40.9000>43.00>70.800	Down	-	-
	2-Ketoglutaric acid	C ₅ H ₆ O ₅	[M-H]	145.0291	72.700>78.600	Up	-	-
	N-Acetylornithine	$C_7H_{14}N_2O_3$	[M+H] ⁺	175.1469	60.043>71.048>74.022	Up	-	_
	3-Methylthiopropyl- desulfoglucosinolate	$C_{11}H_{21}NO_6S_2$	[M-H] ⁻	326.0956	46.9961>59.0139	Up	-	_

frontiersin.org

TABLE 1 Continued

Pathway Putative compound		Predicted formula	Adduct	Parental ion	Fragments	BABA	RBH	JA
	5-Methylthiopentyl glucosinolate	C ₁₃ H ₂₅ NO ₉ S ₃	[M-H] ⁻	434.1026	80.965>111.9710>181.9586	Up	-	-
Phenylalanine; tyrosine; tryptophan biosynthesis	3;4-Dihydroxybenzoic acid	C ₇ H ₆ O ₄	[M+H] ⁺	155.0163	81.0335>109.0284>137.0230	-	Up	-
	Indole-3-glycerol phosphate	C ₁₁ H ₁₄ NO ₆ P	[M+H] ⁺	288.0849	80.9736>118.0651>146.060	-	Down	-
Phenylalanine metabolism	Phenylacetaldehyde	C ₈ H ₈ O	[M-H] ⁻	119.0500	65.039>77.039>91.055	-	Down	-
	Phenylacetic acid	$C_8H_8O_2$	[M-H] ⁻	135.0296	49.136>71.784>76.966	-	Down	-
	8-Methyl-6-nonenoic acid	$C_{10}H_{18}O_2$	[M+H] ⁺	171.1502	41.038>55.054>81.069	-	Up	-
	Benzenecarboxylic acid	C ₇ H ₆ O ₂	[M+H] ⁺	123.0444	83.0861>95.086>113.096	-	Down	-
	4-Vinylphenol	C ₈ H ₈ O	[M-H] ⁻	119.0500	91.054>93.0331>119.049	-	Down	-
	Eugenol	$C_{10}H_{12}O_2$	[M-H]	163.0954	65.039>107.050>121.0295>161.060	-	Down	-
Phenylpropanoid biosynthesis	beta-D-Glucosyl-2-coumarate	C ₁₅ H ₁₈ O ₈	[M-H]	325.0924	117.034>119.050>163.040	-	Down	-
	p-Coumaroyl quinic acid	C ₁₆ H ₁₈ O ₈	[M-H]	337.0774	117.034>119.050>191.056	-	Up	-
	Coniferin	$C_{16}H_{22}O_{8}$	[M-H] ⁻	341.1394	59.013>135.045>339.108	-	Down	-
	4-Imidazolone;	C ₃ H ₄ N ₂ O	[M+H] ⁺	85.0289	42.0338>44.013>55.03	-	Up	-
	Hypoxanthine	C ₅ H ₄ N ₄ O	[M-H] ⁻	135.0296	65.000>92.300>96.900	-	Down	-
	Carbamoyl phosphate	CH ₄ NO ₅ P	[M-H] ⁻	140.0065	78,959	-	Down	-
Purine metabolism	Allantoic acid	$C_4H_8N_4O_4$	[M-H] ⁻	177.0397	76.971>78.970>138.936	-	Up	-
	Deoxyinosine	$C_{10}H_{12}N_4O_4$	[M-H] ⁻	251.1135	107.036>108.0203>135.031	-	Down	-
	Uric acid	$C_{10}H_{12}N_4O_7$	[M-H] ⁻	299.0192	151.025>169.035>197.030	-	Up	-
	Diguanosine tetraphosphate	$C_{20}H_{28}N_{10}O_{21}P_4$	[M-H] ⁻	867.0674	158.9254>442.017>503.972>807.009	-	Down	-
Pyrimidine metabolism	Carbamoyl phosphate	CH ₄ NO ₅ P	[M-H]	140.0065	78,959	-	Down	-
	N-Carbamoyl-L-aspartate	C ₅ H ₈ N ₂ O ₅	[M-H] ⁻	177.0397	41.998>59.02488.039	-	Up	-
	2';3'-Cyclic CMP	$C_9H_{12}N_3O_7P$	[M+H] ⁺	306.0697	113.0541>178.061	-	Down	-
	2'-Deoxycytidine5'- monophosphate	C ₉ H ₁₄ N ₃ O ₇ P	[M+H] ⁺	308.0922	81.033>94.040>112.051	-	Down	-
	(Z)-3-Aminoacrylate	C ₃ H ₅ NO ₂	[M+H] ⁺	88.0759	42.034>52.018>70.029>71.013	Up	_	-
	5-Methyluracil	$C_5H_6N_2O_2$	[M-H] ⁻	125.0240	41.153>41.999	Down	_	-
	Uracil-6-carboxylic acid	$C_5H_4N_2O_4$	[M-H] ⁻	154.9982	41.998>68.0136>85.005	Up	-	-

Ч RBH Down Down Пp $^{\rm Up}$ $^{\rm L}$ Up Пp 12.00>57.900>127.400 17.0335>119.0491>145.0648 57.044>126.029>143.0564 11.998>120.056 17.034>119.050>191.056 59.0463>199.0766>243.070 44.998>65.003>68.050 85.0357>253.0255>255.041 Fragments Parental ion 140.0065 309.0965 299.0192 277.1372 325.0924 337.0774 243.0508 Adduct [M+H] M+H]⁺ [M-H]. M-H] [M-H] [M-H]. [M-H] [M-H]. Predicted formula $C_5H_{10}N_2O_3$ C13H18N4O6 C₁₄H₈N₂O₆ C9H16N4O6 $C_{14}H_{12}O_4$ $C_{19}H_{16}O_{4}$ $C_{16}H_{18}O_{8}$ C₆H₇NO₃ Putative compound 5-Amino-6-(D-ribitylamino J-2-Aminoglutaramic acid 6;7-Dimethyl-8-(D-ribityl) p-Coumaroyl quinic acid Bisdemethoxycurcumin 2-Aminomuconate6-Cinnabarinic acid semialdehyde Picetannol Stilbenoid; diarylheptanoid and gingerol Pathway Tryptophan metabolism Riboflavin metabolism biosynthesis

Continued

metabolites upregulated; Down= metabolites downregulated compared to the corresponding treatment infected condition

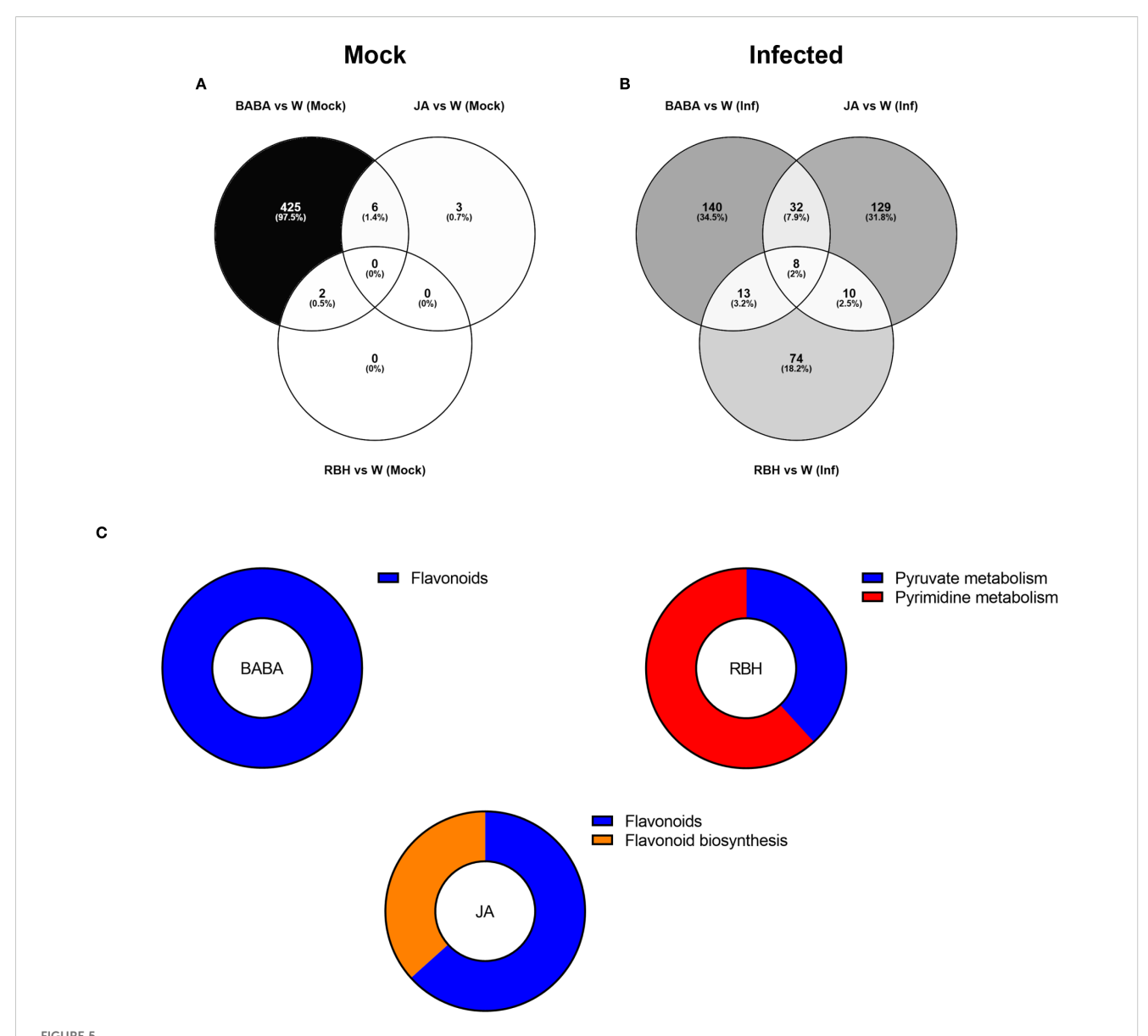
Phenylpropanoid biosynthesis (5 metabolites; 4 down, 1 up), Purine metabolism (7 metabolites; 4 down, 3 up), Pyrimidine metabolism (4 metabolites; 3 down, 1 up), Riboflavin metabolism (2 metabolites; 1 up, 1 down), Stilbenoid biosynthesis (3 metabolites; 2 up, 1 down), and Tryptophan metabolism (2 metabolites; 1 up, 1 down) (Figure 4C; Table 1).

Isolation of direct and priming compounds and primed pathways identification in Soraya

A similar analysis was performed in Soraya. In contrast to Rowena, BABA triggered the most extensive metabolic reprogramming in Soraya under mock conditions, with 503 (97.3%) metabolites induced, whereas RBH and JA affected only 2 (0.4%) and 1 (0.2%) features, respectively (Supplementary Figure 4A). Minimal overlap was observed between treatments, with only 2 metabolites shared between BABA and RBH and 9 metabolites between BABA and JA. Upon *B. cinerea* infection, BABA continued to drive the strongest response, inducing 190 (41.1%) metabolites, followed by JA (103, 22.4%) and RBH (74, 16.1%) (Supplementary Figure 4B). Infected samples showed low shared responses, with 59 features shared between BABA and JA, 15 between BABA and RBH, 8 between JA and RBH, and only 10 features common to all treatments.

Direct-acting metabolites, *i.e.* those uniquely regulated under mock conditions, were predominantly BABA-associated (433), with JA and RBH contributing only 9 and 2 metabolites, respectively (Supplementary Figure 4C) This was also observed when comparing the filtered metabolites, where the dominance of BABA persisted with 425 (97.5%) metabolites remaining specific to this elicitor. In comparison, JA and RBH contributed 3 and 0 metabolites, respectively (Figure 5A).

Priming-associated metabolites (elicitor-induced only in the presence of B. cinerea) revealed more balanced contributions. BABA was associated with 193 features, JA with 179, and RBH with 105 (Supplementary Figure 4C). Comparison of the priming effects by each elicitor revealed 140 metabolites (34.5%) exclusive to BABA, 129 (31.8%) to JA, and 74 (18.2%) to RBH (Figure 5B). The Venn diagram identified 8 metabolites (2%) shared by the three elicitors, 10 (2.5%) shared between JA and RBH, 32 (7.5%) shared between BABA and JA, and 13 (3.2%) shared between BABA and RBH. Pathway enrichment analysis was also performed in Soraya. A total of 16 priming-associated metabolites were putatively identified: 3 specific to BABA, 7 to RBH, and 5 to JA (Table 2). As with Rowena, metabolites were annotated using the KEGG database for Fragaria vesca and an internal reference library, and identifications were confirmed using ChromaLynx and MS spectral matching. Where in-library spectra were unavailable, additional spectral data were sourced from public databases such as PubChem and HMDB. Pathway enrichment analysis revealed that the Flavonoid biosynthesis pathway was significantly enriched for both BABA- and JA-associated priming metabolites, involving 3 metabolites (all upregulated) and 5 metabolites (3 upregulated, 2 downregulated), respectively. In contrast, RBH-primed



Metabolomic responses to elicitor treatments in Soraya. (A) Venn diagram showing the number of metabolites exclusively induced under mock conditions (no infection) by RBH, BABA, and JA in Soraya. (B) Venn diagram showing the number of metabolites exclusively induced under B. cinerea infected conditions by RBH, BABA, or JA in Rowena. Percentages represent each elicitor's contribution to the total number of direct/priming-associated features. The number of shared metabolites between treatments is also indicated. (C) Pathway enrichment of priming-associated metabolites in Rowena. Putatively annotated priming-associated metabolites uniquely induced by BABA and RBH in B. cinerea-infected Soraya plants were subjected to pathway enrichment analysis using the KEGG database for Fragaria vesca and one internal library. Pie charts represent the percentage of statistically significant enriched pathways (p < 0.05) for BABA (left) and RBH (right), based on the number of annotated metabolites per pathway, are shown for each elicitor.

metabolites were enriched in Pyruvate metabolism (4 metabolites all down) and Pyrimidine metabolism (3 metabolites all down) (Figure 5C; Table 2).

Discussion

This study shows that the effectiveness of chemical elicitors in inducing resistance to *B. cinerea* in strawberry is both cultivar- and compound-dependent. Notably, RBH in Rowena and BABA in Soraya led to significant metabolome changes and reduced lesion

development, even in long-term assessments. These findings highlight how cultivar-specific metabolic responses influence induced resistance, providing insight into potential pathways and biomarkers underlying the priming process.

Three commercial strawberry varieties, Durban, Rowena, and Soraya were tested for their capacity to express induced resistance against *B. cinerea*. In strawberry, there are no genotypes fully resistant to *B. cinerea* (Bestfleisch et al., 2015; Petrasch et al., 2019). However, our results highlight differences in basal resistance among the three cultivars and across developmental stages. Durban and Rowena showed persistent susceptibility to *B.*

TABLE 2 Summary of the pathways enriched by BABA, RBH and JA treatment in Soraya and the identified metabolites associated to those pathways.

Pathway	Putative compound	Predicted formula	Adduct	Parental ion	Fragments	BABA	RBH	JA
Flavonoid	Isoquercitrin	$C_{21}H_{20}O_{12}$	[M-H]	463.0877	255.029>284.031>301.071	Up	-	-
	Plantagoside	C ₂₁ H ₂₂ O ₁₂	[M+H] ⁺	467.0796	83.013>151.002>313.0919	Up	-	-
	Nepitrin	C ₂₂ H ₂₂ O ₁₂	[M-H] ⁻	477.1114	201.046>235.061>259.060	Up	-	-
	Epicatechin	C ₁₅ H ₁₄ O ₆	[M-H]	289.0712	109.0287>203.0708>221.0806>289.0712	-	-	Down
Flavonoid biosynthesis	Afzelechin	C ₁₅ H ₁₄ O ₅	$[M+H]^+$	275.1114	105.033>107.0489>139.0381	-	-	Up
	Eriodictyol	C ₁₅ H ₁₂ O ₆	[M+H] ⁺	289.0615	83.013>109.029>245.045	-	-	Up
	Dihydroquercetin	C ₁₅ H ₁₂ O ₇	[M-H]	303.0500	151.0029>287.055	-	-	Down
	p-Coumaroyl quinic acid	C ₁₆ H ₁₈ O ₈	[M-H]	337.0774	117.0346>119.0500>191.0561	-	-	Up
Pyruvate metabolism	Acetic acid	$C_2H_4O_2$	[M-H]	59.0154	41.003>59.013	-	Down	-
	(S)-Lactate	C ₃ H ₆ O ₃	[M-H]	89.0245	53.0026>72.992>89.023	-	Down	-
	2-Butynedioic acid	$C_4H_2O_4$	[M-H]	113.0241	68.998	-	Down	-
	2-Oxobutanedioic acid	$C_4H_4O_5$	[M-H]	131.0345	41.007>43.0184>87.0082	-	Down	-
Pyrimidine metabolism	Carbamide	CH ₄ N ₂ O	[M-H]	59.0151	41.998	-	Down	-
	3-Hydroxypropanoate	C ₃ H ₆ O ₃	[M-H]	89.0244	41.002>59.013>71.013	-	Down	-
	Dihydrouracil	$C_4H_6N_2O_2$	[M-H]	113.0241	41.998>42.034	-	Down	-

Up, metabolites upregulated; Down, metabolites downregulated compared to the corresponding treatment infected condition.

cinerea, while Soraya exhibited greater resilience after the second application (Figure 1; Supplementary Figure 1B). These differences, observed under controlled environmental conditions, suggest a genetic basis for basal resistance rather than an environmental influence.

We tested five chemical elicitors, BABA, RBH, I3CA, JA, and SA, for their capacity to induce resistance. Surprisingly, a single application of any elicitor was insufficient in all cultivars (Supplementary Figure 1A). This lack of induced resistance may be partially explained by the relatively low concentrations used in our study, which fall at the lower end of the ranges reported in successful induced resistance studies (Buswell et al., 2018). It is also likely that intrinsic, cultivar-specific traits modulate the responsiveness to these compounds. Strawberry cultivars exhibit significant variations in both basal and inducible defences, and previous studies have demonstrated differences in elicitor responsiveness among varieties (Seijo et al., 2008). Our findings reinforce the notion that genetic background plays a critical role in shaping immune responses in strawberries.

Neither I3CA nor SA conferred resistance in any of the cultivars. The ineffectiveness of I3CA could be hypothesized to be due to its potential to act more as a downstream marker of defence activation rather than as a true elicitor. Moreover, the lack of SAinduced resistance is not unexpected, as SA is typically associated with defence responses against biotrophic pathogens, whereas B. cinerea is a necrotrophic. The antagonistic crosstalk between the SA and JA signalling pathways often results in SA being ineffective in necrotrophic pathogen resistance (Glazebrook, 2005; Spoel et al., 2007). Interestingly, earlier studies have shown that activation of the SA pathway can suppress JA-mediated responses, thus rendering plants more susceptible to B. cinerea (El Oirdi et al., 2011; Fugate et al., 2013; Ha et al., 2021; Khanam et al., 2005); however, we did not observe this in our experiments. We indeed observed some effects of JA, which significantly reduced lesion size in Durban after the second and third applications, consistent with its welldocumented role in defence against necrotrophic pathogens.

The JA effect did not last after the third application and did not happen in Rowena or Soraya. This suggests that the concentration used may not have been strong enough to produce a strong response. Alternatively, this lack of effectiveness could be due to differences between the plant varieties in how they respond to hormones or how sensitive their receptors are to JA. These underlying factors highlight the complexity of elicitor interactions in strawberry and emphasize the importance of optimizing treatment conditions for each genetic background.

In contrast, RBH and BABA were highly effective in reducing lesion sizes in Rowena and Soraya after four applications, and their effectiveness continued beyond this point. RBH reduced lesion size by 67.5% in Rowena and 64% in Soraya, while BABA reduced lesion size by 41.6% in Rowena. Moreover, long-term resistance was assessed in 18-week-old plants. In Rowena, BABA continued to confer protection, while Soraya retained reduced lesion sizes with both BABA and RBH. This supports the capacity of these compounds to establish durable resistance, potentially through priming mechanisms, and these findings align with previous

reports in tomato and Fragaria vesca (Buswell et al., 2018; Wilkinson et al., 2017). However, BABA has been shown to induce susceptibility rather than resistance in F. vesca, with transcriptional profiling confirming this response (Badmi et al., 2022, 2019). On the contrary, RBH has been demonstrated to induce resistance against B. cinerea in F. vesca, emphasising the differential activity of these compounds across Fragaria species (Badmi et al., 2019). Moreover, long-term induced resistance was also observed in treatments with JA in Soraya, which was unexpected due to the lack of short-term resistance induced by this elicitor in both cultivars. This could be due to a delayed priming imprinting of the effects of the plant hormone, or to the developmental stage of Soraya. Durban showed no response to the elicitor treatments, likely due to genetic or physiological traits limiting its defence activation. Taken together, these results demonstrate the importance of species- and cultivar-specific responses to elicitors, suggesting that optimisation of elicitor use in strawberry will require consideration of both the compound and the cultivar.

None of the elicitors had a significant negative impact on the relative growth rate (RGR), flowering or fruit production, suggesting a low risk of fitness penalties under our treatment conditions. This is particularly relevant for BABA, which has been associated with phytotoxicity and growth suppression in other species at higher doses (van Hulten et al., 2006). In contrast, RBH has shown minimal impact on growth and good systemic movement, supporting its potential use in sustainable agriculture.

Metabolomic analyses confirmed that the efficacy and mode of action of the elicitor are cultivar-dependent. PCA and hierarchical clustering of Water-treated plants revealed clear separation between Rowena and Soraya, independent of infection status (Figure 2B). At 24 hpi, *B. cinerea* had little effect on the global metabolome, demonstrating that cultivar identity was the dominant factor influencing baseline metabolic variation. These metabolomic distinctions may underlie the differential responses to elicitor-induced resistance observed in our study.

Next, we examined the impact of specific elicitors on the metabolome of both varieties (Figure 3). In Rowena, RBH had the most pronounced metabolic impact under both mock and infected conditions, indicating a direct and priming effect. In Rowena, the BABA effect was infection-dependent, suggesting a priming-specific response. In Soraya, however, BABA had strong effects under both conditions, consistent with a mechanism of direct activation. JA exhibited minimal influence on Rowena but did alter the Soraya metabolome during infection, indicating an infection-dependent mode of action.

Venn diagrams and PCA-supported heatmaps revealed that RBH in Rowena and BABA in Soraya triggered the most substantial metabolic shifts (Figures 4, 5). In both cases, these elicitors led to a higher diversity and abundance of priming-associated metabolites, which were correlated with increased resistance phenotypes. This indicates that elicitor efficacy depends on the plant's ability to adjust its metabolism in response to both treatment and pathogen. In Soraya, while the four applications of BABA did not significantly

reduce lesion size, there was a noticeable trend towards improved resistance. Notably, long-term resistance was strongly induced following BABA treatment, suggesting that while the direct activation of defence responses may be transient or subtle, durable priming effects are maintained over time. This supports a model in which BABA acts through sustained priming rather than immediate defence activation in Soraya.

Pathway enrichment analysis provided key insights into elicitor-induced resistance mechanisms (Figures 4, 5). In Rowena, RBH led to significant enrichment in various primary metabolic pathways, including amino acids, nucleotides, cofactors, and vitamins.

Amino acid metabolism was significantly impacted in Rowena, especially in the phenylalanine, tyrosine, and tryptophan pathways, with most metabolites generally downregulated upon RBH treatment. Similarly, enrichment of purine and pyrimidine metabolism also occurred, with most metabolites downregulated. Allantoic acid, uric acid, and 4-imidazolone, within catabolism of purine for storage and transport of nitrogen, were upregulated, suggesting involvement of RBH in nitrogen metabolism (Ohyama et al., 2023; Yang and Han, 2004). The overall downregulation of primary metabolism under RBH treatment may suggest reallocations of energy resources during priming, redirected towards defence pathways (Rojas et al., 2014). Accordingly to our results, amino acid metabolism was found to be suppressed during priming (Schwachtje et al., 2019). Cofactors and vitamins metabolism enriched by RBH in Rowena, included precursors of riboflavin (Vitamin B2), whose efficacy as elicitor of systemic resistance against fungal pathogens (including B. cinerea) relies on activation of Reactive Oxygen Species (ROS) signalling, the lipoxygenase pathway, pathogenesis-related proteins (PR), and defence and antioxidant enzymes such as phenylalanine ammonia lyase (PAL) and peroxidase (POD) (Azami-Sardooei et al., 2010; Boubakri et al., 2013; Zhu et al., 2024). Within secondary metabolism, monoterpenoid and stilbenoid biosynthesis were upregulated by RBH in Rowena. Monoterpenoids can kill the pathogen directly or, due to their volatile properties, act as longdistance signals to trigger defence responses in the distal parts of the plant (Riedlmeier et al., 2017). Stilbenoids' role against B. cinerea has been widely studied, especially for resveratol (Ahn et al., 2015; Xu et al., 2018). In our study, Piceatannol, a hydroxylated derivative of resveratrol, was found to be upregulated. Surprisingly, flavonoid biosynthesis was largely downregulated in Rowena under RBH treatment. Although most of the metabolites in phenylpropanoidlinked pathways were downregulated, p-Coumaroyl quinic acid was the only one upregulated. This metabolite is not only involved as an intermediate in flavonoid and lignin pathways, but also plays a central role in the antioxidant and ROS-scavenging mechanisms (Lee et al., 2013).

Unlike for RBH, BABA-primed Rowena plants showed a comparable enrichment of primary metabolism, particularly with upregulation in amino acid (e.g., histidine, alanine, aspartate, glutamate) and nucleotide (e.g., pyrimidine) metabolism, as well

as 2-oxocarboxylic acid metabolism. Our results support previous findings by Pastor et al. (2014), which demonstrate that the influence of BABA on primary metabolism during the priming phase includes the accumulation of amino acids and enhanced Tricarboxylic acid (TCA) cycle activity. Similarly to Pastor et al. (2014), TCA intermediates, 2-Ketoglutaric acidacid and Fumaric acid, were enriched under BABA treatment. Interestingly, both pyrimidine biosynthesis and degradation pathways were upregulated within nucleotide metabolism, suggesting the maintenance of nucleotide homeostasis. This is notable given that the BABA receptor in Arabidopsis has been identified as an aspartyl-tRNA synthetase, linking BABA perception to amino acid metabolism and protein synthesis (Luna et al., 2014a). Similarly to the effect of RBH, flavonoid and lignan biosynthesis were also enriched, with most flavonoids downregulated and lignans upregulated. During the priming phase, plants can accumulate and store conjugates of compounds that play a role in defences (Pastor et al., 2014). According to this, we found that BABA and RBH induced the enrichment of the glucoside form of quercetin, Isoquercitrin, which is hydrolysed by plant βglucosidases, releasing quercetin, a potent antioxidant, for ROS scavenging of, thereby activating plant immune responses. For instance, pre-treatment with quercetin induced resistance through the SA-dependent signalling pathway in Arabidopsis against Pseudomonas syringae, leading to the conclusion that similar flavonoids (similar to quercetin) may also work (An et al., 2023). Moreover, within flavonoids, also the 5,7-Dihydroxychromone was consistently modulated in BABA- and RBH-treated plants. These results highlight common metabolic signatures for BABA and RBH in Rowena, consistent with an earlier study (Buswell et al., 2018) and reinforce the idea that both compounds activate similar metabolic pathways to improve resistance in this cultivar.

In conclusion, as a priming agent, RBH in Rowena suppresses primary metabolism at the early stage of the infection and induces selective secondary metabolism (upregulation of stilbenoids and monoterpenoids). At the same time, BABA has a broader metabolic impact, especially on upregulation of primary metabolism, and induces selective secondary metabolism (upregulation of lignanes). These results highlight different finetuning metabolic reprogramming performed by RBH and BABA in Rowena.

In Soraya, pathway enrichment analyses revealed distinct metabolomic signatures for each elicitor. BABA-primed metabolites were mainly enriched in flavonoid biosynthesis. Specifically, several flavonol glycosides, including Isoquercitrin, Plantagoside, and Nepitrin, were upregulated. Enrichment of Isoquercitrin in BABA-treated Rowena and RBH-treated Soraya suggests a potential role as a conserved marker of elicitor responsiveness. JA-priming in Soraya also affected flavonoid metabolism. While some precursors, such as Eriodictyol and compounds like Afzelechin and p-Coumaroyl quinic acid, were upregulated, key flavonoids such as Epicatechin and its precursor Dihydroquercetin were downregulated, indicating a complex

regulation of this pathway during JA-induced priming. Moreover, RBH-primed Soraya plants showed downregulation of primary metabolic pathways, including nucleotide (e.g., pyrimidine) and carbohydrate (e.g., pyruvate) metabolism. The downregulation of pyruvate metabolism may reflect energy conservation strategies associated with priming. Similarly, suppression of pyrimidine degradation pathways, which are crucial for nucleotide recycling and homeostasis, may represent a stress-mediated reprogramming strategy that contributes to effective resistance. Overall, the differential modulation of energy-related and defence-associated pathways illustrates how elicitor-induced priming operates through cultivar-specific metabolic adaptations.

Together, our results show that BABA, RBH, and JA induce distinct metabolomic reprogramming depending on the cultivar. While RBH suppresses primary metabolism but activates different secondary pathways in both cultivars, BABA elicits primary metabolism in Rowena and secondary metabolism in Soraya. The JA effect is weak and absent in Rowena but present in Soraya. The lack of observed growth penalties further highlights the potential of these elicitors in sustainable disease management strategies for strawberry. While this study focused on leaf responses to elicitor treatments, we acknowledge that B. cinerea is a major pathogen of strawberry fruit. Leaves were selected as the target organ for metabolomic analysis due to their uniformity and accessibility for early defence monitoring. However, future studies, particularly the ones under field conditions (greenhouse or open field) should complement the leaf assessment with fruit collected from plants grown under field conditions, to evaluate the efficacy of induced resistance in the most agronomically relevant organs. Nevertheless, this study provides a comprehensive metabolomic view of defence priming induced by BABA, RBH, and JA in commercial strawberry cultivars. By integrating phenotypic and metabolomic data, we reveal how cultivar-specific responses and metabolic reprogramming influence the efficacy of elicitors. These insights can inform the strategic deployment of chemical elicitors in strawberry breeding and disease management programs to combat B. cinerea in a sustainable way.

Data availability statement

The datasets presented in this study can be found in online repositories. The names of the repository/repositories and accession number(s) can be found in the article.

Author contributions

CM: Data curation, Formal analysis, Investigation, Software, Validation, Visualization, Writing – original draft. VP: Data curation, Formal analysis, Investigation, Methodology, Writing – review & editing. TF: Conceptualization, Funding acquisition, Resources, Supervision, Writing – review & editing. SC: Conceptualization, Funding acquisition, Resources, Supervision, Writing – review & editing. EL: Conceptualization, Methodology, Resources, Supervision, Writing – original draft.

Funding

The author(s) declare financial support was received for the research and/or publication of this article. The authors would like to thank the Foundation for Science and Technology (FCT) for funding CM Ph.D. scholarship (2021.06641.BD) and the R&D Project 'Botrytis-XTalk' (PTDC/ASP-PLA/4478/2021) to TRF and SMPC. TRF acknowledges FCT for funding through CEECInst LA (https://doi.org/10.54499/CEECINSTLA/00037/2022/CP2992/CT0001). This research was also supported by national funds via FCT through the Strategic Projects UIDB/05748/2025 and UIDP/05748/2025. The work was also supported by the BBSRC Future Leader Fellowship (BB/P00556X/2) and the pump-priming funding received by the Horticultural Quality and Food Loss Network (WXA3189N/P16188/UoB_Luna-Diez) to EL.

Acknowledgments

We also thank the Servicio de Instrumentación Científica (SCIC) at UJI for its technical support and the project CI AICO/2021/092 from the Generalitat Valenciana. We also thank Lamya Majeed for the technical experimental support to CM and to Saturn Bioponics for providing the commercial strawberry cultivars.

Conflict of interest

The authors declare that the research was conducted in the absence of any commercial or financial relationships that could be construed as a potential conflict of interest.

The author(s) declared that they were an editorial board member of Frontiers, at the time of submission. This had no impact on the peer review process and the final decision.

Generative AI statement

The author(s) declare that Generative AI was used in the creation of this manuscript. The authors verify and take full responsibility for the use of generative AI in the preparation of this manuscript. Generative AI (ChatGPT, OpenAI) was used to support the writing and editing process of this manuscript. Specifically, the tool was employed to: - Refine the clarity, grammar, and flow of text in the Introduction, Results, and Discussion sections. - Improve the readability and conciseness of scientific language, while ensuring accuracy of terminology. - Assist in restructuring paragraphs to improve logical coherence and alignment with journal style. - Generate suggestions for figure legends, running titles, scope statements, and author contribution narratives based on provided content. - Draft the initial version of the abstract and rephrase sections as per the authors' detailed inputs and data. At no point was generative AI used to generate original scientific content, analyse data, or interpret experimental results. All scientific insights, conclusions, and interpretations are the result of

the authors' own expertise and evaluation. The authors have reviewed, edited, and approved all AI-assisted content to ensure it reflects the scientific integrity and objectives of the study.

Any alternative text (alt text) provided alongside figures in this article has been generated by Frontiers with the support of artificial intelligence and reasonable efforts have been made to ensure accuracy, including review by the authors wherever possible. If you identify any issues, please contact us.

Publisher's note

All claims expressed in this article are solely those of the authors and do not necessarily represent those of their affiliated organizations, or those of the publisher, the editors and the reviewers. Any product that may be evaluated in this article, or claim that may be made by its manufacturer, is not guaranteed or endorsed by the publisher.

Supplementary material

The Supplementary Material for this article can be found online at: https://www.frontiersin.org/articles/10.3389/fpls.2025.1675649/full#supplementary-material

SUPPLEMENTARY FIGURE 1

Lesion development in strawberry cultivars during early elicitor applications. Lesion diameter in Durban, Rowena, and Soraya after the first (A), second (B), and third **(C)** elicitor applications at 6, 8, and 10 weeks of plant age, respectively. Inoculations were performed five days after each treatment application. Boxplots represent lesion diameter (mm) with the median line, interquartile range (boxes), and whiskers extending to the minimum and maximum values. Each point represents biological replicates (individual plants) (n = 8-12 per treatment). Capital letters indicate statistical differences between the Water treatments of each variety. Lowercase letters indicate statistically significant differences between elicitors within each variety (One-way ANOVA followed by Tukey's post hoc test or Welch's ANOVA followed by Dunnett's T3; p < 0.05; n = 8-12).

SUPPLEMENTARY FIGURE 2

Assessment of growth following elicitor treatments. Relative Growth Rate (RGR) was calculated based on leaf area expansion between weeks 11 and 14 using ImageJ software. Boxplots represent RGR (cm² week-¹) with the median line, interquartile range (boxes), and whiskers extending to the minimum and maximum values. Each point represents biological replicates (individual plants). ns indicates not significant differences (One-way ANOVA; p < 0.05; n = 8-12).

SUPPLEMENTARY FIGURE 3

Metabolite reprogramming in Rowena in response to elicitors. (A) Venn diagram showing metabolites induced under mock condition by BABA, RBH, and JA in Rowena. (B) Venn diagram showing metabolites induced under B. cinerea infected condition. (C) Filtering of mock- (blue circles) and infection (yellow circles)-specific metabolites for each treatment. The diagram separates direct (mock-only) and priming (infection-only) responses, prior to exclusive grouping in Figure 4.

SUPPLEMENTARY FIGURE 4

Metabolite reprogramming in Soraya in response to elicitors. (A) Venn diagram showing metabolites induced under mock condition by BABA, RBH, and JA in Soraya. (B) Venn diagram showing metabolites induced under B. cinerea infected condition. (C) Filtering of mock- (blue circles) and infection (yellow circles)-specific metabolites for each treatment. The diagram separates direct (mock-only) and priming (infection-only) responses, prior to exclusive grouping in Figure 5.

References

Ahn, S. Y., Kim, S. A., and Yun, H. K. (2015). Inhibition of *Botrytis cinerea* and accumulation of stilbene compounds by light-emitting diodes of grapevine leaves and differential expression of defense-related genes. *Eur. J. Plant Pathol.* 143, 753–765. doi: 10.1007/s10658-015-0725-5

An, J., Kim, S. H., Bahk, S., Le Anh Pham, M., Park, J., Ramadany, Z., et al. (2023). Quercetin induces pathogen resistance through the increase of salicylic acid biosynthesis in *Arabidopsis*. *Plant Signal Behav*. 18, 2270835. doi: 10.1080/15592324.2023.2270835

Azami-Sardooei, Z., França, S., Vleesschauwer, D., and Höfte, M. (2010). Riboflavin induces resistance against *Botrytis cinerea* in bean, but not in tomato, by priming for a hydrogen peroxide-fueled resistance response. *Physiol. Mol. Plant Pathol.* 75, 23–29. doi: 10.1016/j.pmpp.2010.08.001

Babalar, M., Asghari, M., Talaei, A., and Khosroshahi, A. (2007). Effect of pre- and postharvest salicylic acid treatment on ethylene production, fungal decay and overall quality of *Selva* strawberry fruit. *Food Chem.* 105, 449–453. doi: 10.1016/j.foodchem.2007.03.021

Badmi, R., Tengs, T., Brurberg, M. B., Elameen, A., Zhang, Y., Haugland, L. K., et al. (2022). Transcriptional profiling of defense responses to *Botrytis cinerea* infection in leaves of *Fragaria vesca* plants soil-drenched with beta-aminobutyric acid. *Front. Plant Sci.* 13. doi: 10.3389/fpls.2022.1025422

Badmi, R., Zhang, Y., Tengs, T., Brurberg, M. B., Krokene, P., Fossdal, C. G., et al. (2019). Induced and primed defence responses of Fragaria vesca to Botrytis cinerea infection. Preprint. *BioRxiv*. doi: 10.1101/692491

Bestfleisch, M., Luderer-Pflimpfl, M., Höfer, M., Schulte, E., Wünsche, J. N., Hanke, M.-V., et al. (2015). Evaluation of strawberry (*Fragaria L.*) genetic resources for resistance to *Botrytis cinerea*. *Plant Pathol.* 64, 396–405. doi: 10.1111/ppa.12278

Bi, K., Liang, Y., Mengiste, T., and Sharon, A. (2023). Killing softly: a roadmap of *Botrytis cinerea* pathogenicity. *Trends Plant Sci.* 28, 211–222. doi: 10.1016/j.tplants.2022.08.024

Boubakri, H., Chong, J., Poutaraud, A., Schmitt, C., Bertsch, C., Mliki, A., et al. (2013). Riboflavin (Vitamin B2) induces defence responses and resistance to *Plasmopara viticola* in grapevine. *Eur. J. Plant Pathol.* 136, 837–855. doi: 10.1007/s10658-013-0211-x

Buswell, W., Schwarzenbacher, R. E., Luna, E., Sellwood, M., Chen, B., Flors, V., et al. (2018). Chemical priming of immunity without costs to plant growth. *New Phytol.* 218, 1205–1216. doi: 10.1111/nph.15062

Catoni, M., Alvarez-Venegas, R., Worrall, D., Holroyd, G., Barraza, A., Luna, E., et al. (2022). Long-lasting defence priming by beta-aminobutyric acid in tomato is marked by genome-wide changes in DNA methylation. *Front. Plant Sci.* 13. doi: 10.3389/fbls.2022.836326

Chambers, M. C., Maclean, B., Burke, R., Amodei, D., Ruderman, D. L., Neumann, S., et al. (2012). A cross-platform toolkit for mass spectrometry and proteomics. *Nat. Biotechnol.* 30, 918–920. doi: 10.1038/nbt.2377

Chen, S. N., Luo, C. X., Hu, M. J., and Schnabel, G. (2016). Fitness and competitive ability of *botrytis cinerea* isolates with resistance to multiple chemical classes of fungicides. *Phytopathology* 106, 997–1005. doi: 10.1094/PHYTO-02-16-0061-R

Csikász-Krizsics, A., Mátai, A., Nagy, Á., Kovács, S., Végh, B., Werner, J., et al. (2013). BABA (β -aminobutyric acid) induced resistance against grey mould and virus infection in grapevine. *Proc. Int. Org. Biol. Control. (IOBC)* 89, 429–432.

De Kesel, J., Conrath, U., Flors, V., Luna, E., Mageroy, M. H., Mauch-Mani, B., et al. (2021). The induced resistance lexicon: do's and don'ts. *Trends Plant Sci.* 26, 685–691. doi: 10.1016/j.tplants.2021.01.001

El Oirdi, M., El Rahman, T. A., Rigano, L., El Hadrami, A., Rodriguez, M. C., Daayf, F., et al. (2011). *Botrytis cinerea* manipulates the antagonistic effects between immune pathways to promote disease development in tomato. *Plant Cell* 23, 2405–2421. doi: 10.1105/tpc.111.083394

FAO, U. W., and WOAH (2023). One Health and the United Nations Sustainable Development cooperation Framework. Guidance for United Nations country teams

(Rome: Food and Agriculture Organization of the United Nations (FAO)). doi: 10.4060/cc5067en

Faretra, F., and Pollastro, S. (1991). Genetic basis of resistance to benzimidazole and dicarboximide fungicides in *Botryotinia fuckeliana* (*Botrytis cinerea*). *Mycol. Res.* 95, 943–951. doi: 10.1016/S0953-7562(09)80091-9

Fugate, K. K., Ferrareze, J. P., Bolton, M. D., Deckard, E. L., Campbell, L. G., and Finger, F. L. (2013). Postharvest salicylic acid treatment reduces storage rots in water-stressed but not unstressed sugarbeet roots. *Postharvest. Biol. Technol.* 85, 162–166. doi: 10.1016/j.postharvbio.2013.06.005

Gamir, J., Pastor, V., Cerezo, M., and Flors, V. (2012). Identification of indole-3-carboxylic acid as mediator of priming against *Plectosphaerella cucumerina*. *Plant Physiol. Biochem.* 61, 169–179. doi: 10.1016/j.plaphy.2012.10.004

Gamir, J., Pastor, V., Kaever, A., Cerezo, M., and Flors, V. (2014). Targeting novel chemical and constitutive primed metabolites against *Plectosphaerella cucumerina*. *Plant J.* 78, 227–240. doi: 10.1111/tpj.12465

Ghozlan, M. H., El-Argawy, E., Tokgöz, S., Lakshman, D. K., and Mitra, A. (2020). Plant defense against necrotrophic pathogens. *Am. J. Plant Sci.* 11, 2122–2138. doi: 10.4236/ajps.2020.1112149

Glazebrook, J. (2005). Contrasting mechanisms of defense against biotrophic and necrotrophic pathogens. *Annu. Rev. Phytopathol.* 43, 205–227. doi: 10.1146/annurev.phyto.43.040204.135923

Ha, S. T. T., Kim, Y. T., Jeon, Y. H., Choi, H. W., and In, B. C. (2021). Regulation of botrytis cinerea infection and gene expression in cut roses by using nano silver and salicylic acid. Plants (Basel). 10. doi: 10.3390/plants10061241

Hassan, E. A., Mostafa, Y. S., Alamri, S., Hashem, M., and Nafady, N. A. (2021). Biosafe management of *botrytis* grey mold of strawberry fruit by novel bioagents. *Plants* (*Basel*). 10. doi: 10.3390/plants10122737

He, Z., Webster, S., and He, S. Y. (2022). Growth-defense trade-offs in plants. *Curr. Biol.* 32, R634–r639. doi: 10.1016/j.cub.2022.04.070

Kaever, A., Landesfeind, M., Feussner, K., Mosblech, A., Heilmann, I., Morgenstern, B., et al. (2015). MarVis-Pathway: integrative and exploratory pathway analysis of non-targeted metabolomics data. *Metabolomics* 11, 764–777. doi: 10.1007/s11306-014-0734-v

Kaever, A., Lingner, T., Feussner, K., Göbel, C., Feussner, I., and Meinicke, P. (2009).MarVis: a tool for clustering and visualization of metabolic biomarkers. BMC Bioinf.10, 92. doi: 10.1186/1471-2105-10-92

Khanam, N. N., Ueno, M., Kihara, J., Honda, Y., and Arase, S. (2005). Suppression of red light-induced resistance in broad beans to *Botrytis cinerea* by salicylic acid. *Physiol. Mol. Plant Pathol.* 66, 20–29. doi: 10.1016/j.pmpp.2005.03.006

Koen, E., Trapet, P., Brulé, D., Kulik, A., Klinguer, A., Atauri-Miranda, L., et al. (2014). β -Aminobutyric acid (BABA)-induced resistance in *Arabidopsis thaliana*: link with iron homeostasis. *MPMI* 27, 1226–1240. doi: 10.1094/mpmi-05-14-0142-r

Koo, Y. M., Heo, A. Y., and Choi, H. W. (2020). Salicylic acid as a safe plant protector and growth regulator. *Plant Pathol. J.* 36, 1–10. doi: 10.5423/PPJ.RW.12.2019.0295

Lee, Y. G., Cho, J.-Y., Kim, C.-M., Lee, S.-H., Kim, W.-S., Jeon, T.-I., et al. (2013). Coumaroyl quinic acid derivatives and flavonoids from immature pear (*Pyrus pyrifolia nakai*) fruit. *Food Sci. Biotechnol.* 22, 803–810. doi: 10.1007/s10068-013-0148-z

Li, L., and Zou, Y. (2017). Induction of disease resistance by salicylic acid and calcium ion against *Botrytis cinerea* in tomato (*Lycopersicon esculentum*). *Emir. J. Food Agric.* 29. doi: 10.9755/ejfa.2016-10-1515

Liao, C. J., Hailemariam, S., Sharon, A., and Mengiste, T. (2022). Pathogenic strategies and immune mechanisms to necrotrophs: Differences and similarities to biotrophs and hemibiotrophs. *Curr. Opin. Plant Biol.* 69, 102291. doi: 10.1016/j.pbi.2022.102291

Luna, E. (2016). Using green <I>Vaccination</I> to brighten the agronomic future. Outlooks. Pest Manage. 27, 136–140. doi: $10.1564/v27_jun_10$

Luna, E., Beardon, E., Ravnskov, S., Scholes, J., and Ton, J. (2016). Optimizing chemically induced resistance in tomato against *botrytis cinerea*. *Plant Dis.* 100, 704–710. doi: 10.1094/PDIS-03-15-0347-RE

Luna, E., Flandin, A., Cassan, C., Prigent, S., Chevanne, C., Kadiri, C. F., et al. (2020). Metabolomics to exploit the primed immune system of tomato fruit. *Metabolites* 10. doi: 10.3390/metabo10030096

Luna, E., López, A., Kooiman, J., and Ton, J. (2014b). Role of NPR1 and KYP in long-lasting induced resistance by β -aminobutyric acid. Front. Plant Sci. Volume 5. doi: 10.3389/fpls.2014.00184

Luna, E., van Hulten, M., Zhang, Y., Berkowitz, O., López, A., Pétriacq, P., et al. (2014a). Plant perception of β -aminobutyric acid is mediated by an aspartyl-tRNA synthetase. *Nat. Chem. Biol.* 10, 450–456. doi: 10.1038/nchembio.1520

Martinez-Medina, A., Flors, V., Heil, M., Mauch-Mani, B., Pieterse, C. M. J., Pozo, M. J., et al. (2016). Recognizing plant defense priming. *Trends Plant Sci.* 21, 818–822. doi: 10.1016/j.tplants.2016.07.009

Mauch-Mani, B., Baccelli, I., Luna, E., and Flors, V. (2017). Defense priming: an adaptive part of induced resistance. *Annu. Rev. Plant Biol.* 68, 485–512. doi: 10.1146/annurev-arplant-042916-041132

Mekawi, E. M., Khafagi, E. Y., and Abdel-Rahman, F. A. (2019). Effect of pre-harvest application with some organic acids and plant oils on antioxidant properties and

resistance to *Botrytis cinerea* in pepper fruits. *Sci. Hortic.* 257. doi: 10.1016/j.scienta.2019.108736

Ohyama, T., Matsumoto, K., Goto, H., Saito, A., and Higuchi, K. (2023). Nitrogen metabolism in non-nodulated and nodulated soybean plants related to ureide synthesis. *Nitrogen* 4, 209–222. doi: 10.3390/nitrogen4020014

Oliveros, J. C. (2007-2015). enny. An interactive tool for comparing lists with Venn's diagrams. Available online at: https://bioinfogp.cnb.csic.es/tools/venny/index.html (Accessed July 17, 2025).

Pang, Z., Lu, Y., Zhou, G., Hui, F., Xu, L., Viau, C., et al. (2024). MetaboAnalyst 6.0: towards a unified platform for metabolomics data processing, analysis and interpretation. *Nucleic Acids Res.* 52, W398–W406. doi: 10.1093/nar/gkae253

Pastor, V., Balmer, A., Gamir, J., Flors, V., and Mauch-Mani, B. (2014). Preparing to fight back: generation and storage of priming compounds. *Front. Plant Sci. Volume* 5. doi: 10.3389/fpls.2014.00295

Pastor, V., Luna, E., Mauch-Mani, B., Ton, J., and Flors, V. (2013). Primed plants do not forget. *Environ. Exp. Bot.* 94, 46–56. doi: 10.1016/j.envexpbot.2012.02.013

Petrasch, S., Knapp, S. J., van Kan, J. A. L., and Blanco-Ulate, B. (2019). Grey mould of strawberry, a devastating disease caused by the ubiquitous necrotrophic fungal pathogen *Botrytis cinerea*. *Mol. Plant Pathol.* 20, 877–892. doi: 10.1111/mpp.12794

Polyakovskii, S. A., Kravchuk, Z. N., and Dmitriev, A. P. (2008). Mechanism of action of the plant resistance inducer β -aminobutyric acid in *Allium cepa. Cytol. Genet.* 42, 369–372. doi: 10.3103/s0095452708060029

R Core Team (2024). R: A Language and Environment for Statistical Computing (Vienna, Austria: R Foundation for Statistical Computing). Available online at: https://www.Rproject.org/ (Accessed July 17, 2025).

Rhainds, M., Kovach, J., and Loeb, G. (2002). Impact of strawberry cultivar and incidence of pests on yield and profitability of strawberries under conventional and organic management systems. *Biol. Agric. Hortic.* 19, 333–353. doi: 10.1080/01448765.2002.9754937

Riedlmeier, M., Ghirardo, A., Wenig, M., Knappe, C., Koch, K., Georgii, E., et al. (2017). Monoterpenes support systemic acquired resistance within and between plants. *Plant Cell* 29, 1440–1459. doi: 10.1105/tpc.16.00898

Rojas, C. M., Senthil-Kumar, M., Tzin, V., and Mysore, K. (2014). Regulation of primary plant metabolism during plant-pathogen interactions and its contribution to plant defense. *Front. Plant Sci.* 5 - 2014. doi: 10.3389/fpls.2014.00017

Schneider, C. A., Rasband, W. S., and Eliceiri, K. W. (2012). NIH Image to Image]: 25 years of image analysis. *Nat. Methods* 9, 671–675. doi: 10.1038/nmeth.2089

Schwachtje, J., Whitcomb, S. J., Firmino, A. A. P., Zuther, E., Hincha, D. K., and Kopka, J. (2019). Induced, imprinted, and primed responses to changing environments: does metabolism store and process information? *Front. Plant Sci.* 10. doi: 10.3389/fpls.2019.00106

Seijo, T., Chandler, C., Mertely, J., Moyer, C., and Peres, N. (2008). Resistance of strawberry cultivars and advanced selections to anthracnose and *botrytis* fruit rots. *Proc. Florida State. Hortic. Soc.* 121.

Spoel, S. H., Johnson, J. S., and Dong, X. (2007). Regulation of tradeoffs between plant defenses against pathogens with different lifestyles. *Proc. Natl. Acad. Sci. U.S.A.* 104, 18842–18847. doi: 10.1073/pnas.0708139104

Stevens, K., Roberts, M. R., Jeynes-Cupper, K., Majeed, L., Pastor, V., Catoni, M., et al. (2025). Developmentally regulated generation of a systemic signal for long-lasting defence priming in tomato. *New Phytol.* 245, 1145–1157. doi: 10.1111/nph.20288

Thevenet, D., Pastor, V., Baccelli, I., Balmer, A., Vallat, A., Neier, R., et al. (2017). The priming molecule β -aminobutyric acid is naturally present in plants and is induced by stress. *New Phytol.* 213, 552–559. doi: 10.1111/nph.14298

Ton, J., and Mauch-Mani, B. (2004). Beta-amino-butyric acid-induced resistance against necrotrophic pathogens is based on ABA-dependent priming for callose. *Plant J.* 38, 119–130. doi: 10.1111/j.1365-313X.2004.02028.x

van Hulten, M., Pelser, M., van Loon, L. C., Pieterse, C. M., and Ton, J. (2006). Costs and benefits of priming for defense in *Arabidopsis. Proc. Natl. Acad. Sci. U.S.A.* 103, 5602–5607. doi: 10.1073/pnas.0510213103

Wang, K., Liao, Y., Xiong, Q., Kan, J., Cao, S., and Zheng, Y. (2016). Induction of Direct or Priming Resistance against *Botrytis cinerea* in Strawberries by beta-Aminobutyric Acid and Their Effects on Sucrose Metabolism. *J. Agric. Food Chem.* 64, 5855–5865. doi: 10.1021/acs.jafc.6b00947

Wilkinson, S. W., Pastor, V., Paplauskas, S., Pétriacq, P., and Luna, E. (2017). Longlasting β -aminobutyric acid-induced resistance protects tomato fruit against *Botrytis cinerea*. *Plant Pathol.* 67, 30–41. doi: 10.1111/ppa.12725

Williamson, B., Tudzynski, B., Tudzynski, P., and van Kan, J. A. (2007). *Botrytis cinerea*: the cause of grey mould disease. *Mol. Plant Pathol.* 8, 561–580. doi: 10.1111/j.1364-3703.2007.00417.x

Worrall, D., Holroyd, G. H., Moore, J. P., Glowacz, M., Croft, P., Taylor, J. E., et al. (2012). Treating seeds with activators of plant defence generates long-lasting priming of resistance to pests and pathogens. *New Phytol.* 193, 770–778. doi: 10.1111/j.1469-8137.2011.03987.x

Xu, D., Yu, G., Xi, P., Kong, X., Wang, Q., Gao, L., et al. (2018). Synergistic Effects of Resveratrol and Pyrimethanil against *Botrytis cinerea* on Grape. *Molecules* 23, 1455. doi: 10.3390/molecules23061455

Yang, J., and Han, K. H. (2004). Functional characterization of allantoinase genes from *Arabidopsis* and a nonureide-type legume black locust. *Plant Physiol.* 134, 1039–1049. doi: 10.1104/pp.103.034637

Zhu, M., Yang, Z., Wang, N., Chen, L., Xiao, Y., Yu, L., et al. (2024). Riboflavin alleviates the occurrence of anthracnose caused by *Colletotrichum gloeosporioides* in

postharvest mango and the possible mechanisms involved. Food Biosci. 59, 104169. doi: 10.1016/j.fbio.2024.104169

Zimmerli, L., Métraux, J. P., and Mauch-Mani, B. (2001). beta-Aminobutyric acid-induced protection of *Arabidopsis* against the necrotrophic fungus *Botrytis cinerea*. *Plant Physiol.* 126, 517–523. doi: 10.1104/pp.126.2.517